Available online at www.sciencedirect.com
ScienceDirect
Journal of Computational and Applied Mathematics 205 (2007) 207–230
JOURNAL OF COMPUTATIONAL AND APPLIED MATHEMATICS
www.elsevier.com/locate/cam

The splitting finite-difference time-domain methods for Maxwell's equations in two dimensions

Liping Gao[a], Bo Zhang[a, b, *], Dong Liang[c]

[a] *Department of Mathematical Sciences, Faculty of Engineering and Computing, Coventry University, Coventry CV1 5FB, UK*
[b] *Institute of Applied Mathematics, Chinese Academy of Sciences, Beijing 100080, China*
[c] *Department of Mathematics and Statistics, York University, 4700 Keele Street, Toronto, Ont., Canada M3J 1P3*

Received 6 January 2006; received in revised form 24 April 2006

Abstract

In this paper, we consider splitting methods for Maxwell's equations in two dimensions. A new kind of splitting finite-difference time-domain methods on a staggered grid is developed. The corresponding schemes consist of only two stages for each time step, which are very simple in computation. The rigorous analysis of the schemes is given. By the energy method, it is proved that the scheme is unconditionally stable and convergent for the problems with perfectly conducting boundary conditions. Numerical dispersion analysis and numerical experiments are presented to show the efficient performance of the proposed methods. Furthermore, the methods are also applied to solve a scattering problem successfully.

MSC: 65N10; 65N15

Keywords: Maxwell's equations; Splitting scheme; Finite-difference time-domain; Staggered grid; Stability; Convergence; Perfectly conducting; Scattering; Perfectly matched layer

1. Introduction

Alternating direction implicit methods (ADI) are conventional and efficient numerical methods to solve multi-dimensional problems. It was originally introduced by Peaceman, Douglas and Rachford in 1950s (see [12,4]) for heat flow equations in two dimensions and was later applied extensively in many numerical approximation problems [1–3]. Since the corresponding coefficient matrix of the algebraic system for each iteration in the actual work comes from a one-dimensional problem, the methods save much computer memory and CPU time. Recently, Douglas et al. [3] proposed a way of reducing the perturbation errors caused by the ADI method.

On the other hand, the finite-difference time-domain (FDTD) method (also called Yee's Scheme) for Maxwell's equations, which was first proposed by Yee [17] in 1966 and later developed by Taflove and others [14,15], is a very efficient numerical algorithm in computational electromagnetics. The scheme has been applied in a broad range of problems (for its merit and application see [15]). However, the Yee scheme is only conditionally stable so that for the two-dimensional

* Corresponding author. Institute of Applied Mathematics, Chinese Academy of Sciences, Beijing 100080, China. Fax: +86 10 6254 1689.
E-mail addresses: l.gao@coventry.ac.uk (L. Gao), b.zhang@amt.ac.cn, b.zhang@conventry.ac.uk (B. Zhang), dliang@mathstat.yorku.ca (D. Liang).

0377-0427/$ - see front matter © 2006 Elsevier B.V. All rights reserved.
doi:10.1016/j.cam.2006.04.051

problem, the time step size Δt and the spatial step sizes Δx and Δy should satisfy the Courant–Friedrichs–Lewy (CFL) stability condition

$$c_{\max}\Delta t \leqslant [1/(\Delta x)^2 + 1/(\Delta y)^2]^{-1/2},$$

where $c_{\max}$ is the maximum of the wave velocity $c(x, y) = 1/(\mu\varepsilon)^{-1/2}$ (see [14,15]; note that [14] was the first publication of the correct CFL stability limit for FDTD). Hence, when the spatial step sizes become very small, the computation of the Maxwell equations by Yee's scheme will need much CPU time. Combining Yee's scheme with the ADI time-marching technique would overcome this deficiency. In fact, such work has been discussed in the early 1984s for the two-dimensional problems [8], but, the scheme proposed in [8] was proved to be difficult for obtaining the unconditional stability property for the general three-dimensional Maxwell equations. A unconditionally stable ADI-FDTD scheme was first proposed in [21] for the three-dimensional Maxwell equations with an isotropic, lossless medium, which consists of only two stages for each time step. A detailed analysis of accuracy and dispersion of this ADI-FDTD scheme was carried out in [6,20]. A rigorous error estimate of this ADI-FDTD scheme was given in [5] in the case of perfectly conducting boundary conditions, employing the discrete energy method.

Recently, Namiki [10] proposed a kind of ADI-FDTD schemes for the two-dimensional Maxwell equations with an isotropic, lossless medium. It was proved in [10,18] using the Fourier method that this scheme is unconditionally stable and has reasonable numerical dispersion errors. The method has been successfully applied to solve problems of a monopole antenna near a thin dielectric wall, a strip line with narrow gap, and a perfectly matched layer (PML) problem (see [11,7]).

In this paper, we study effective splitting numerical methods for Maxwell's equations. Combining the splitting technique and the staggered grid, a splitting finite-difference time-domain method (called S-FDTDI) is proposed for the two-dimensional problem. We present a rigorous analysis of the method concerning stability, convergence as well as numerical dispersion and dissipation. By using the energy method it is proved that the S-FDTDI scheme is unconditionally stable and convergent with first order in time and second order in space for the case with perfectly electric conducting (PEC) boundary conditions. The dissipation analysis shows that the S-FDTDI scheme is a first-order perturbation to the Crank–Nicolson (CN) scheme where the perturbation error dominates the truncation error. In order to improve the accuracy of the S-FDTDI scheme, we propose an improved splitting finite-difference time-domain method (called S-FDTDII) for the two-dimensional problem by reducing the perturbation error. The scheme is equivalent to a second-order perturbation of the CN scheme. The two proposed schemes, which are different from the one presented in [10], are much simpler and consist of only two equations at each stage, while each stage of the scheme in [10] has three equations. This feature brings much convenience in practical computation, especially, in the simulation of scattering problems with PML boundary conditions, and will save much more CPU time. To investigate the numerical dispersion error of the two new schemes, the numerical dispersion relations are derived using a simple method. Numerical dispersion relations show that these two schemes are very effective and that the S-FDTDII scheme has less dispersion error than the S-FDTDI scheme has. Numerical experiments of solving the two-dimensional Maxwell equations are presented to show the excellent performance of the proposed methods. The new methods have also been applied to solve a scattering problem with PML boundary conditions, and effective numerical results are obtained.

The remaining part of the paper is organized as follows. In Section 2, the S-FDTDI scheme is proposed for the two-dimensional Maxwell equations. The improved splitting scheme S-FDTDII is also proposed by reducing the perturbation error of the S-FDTDI. In Section 3, we give a rigorous stability and convergence analysis of the S-FDTDI scheme. Numerical dispersion relations as well as numerical dispersion errors are analyzed in Section 4. In Section 5, numerical experiments are presented for solving the Maxwell equations with a PEC boundary condition and a scattering problem with a PML boundary condition.

2. The Maxwell equations and the splitting schemes

In this section, we propose two splitting finite-difference time-domain (S-FDTD) schemes for the two-dimensional Maxwell equations. Based on a splitting technique and staggered grids, the S-FDTDI scheme is proposed first for the problem. To improve the accuracy of S-FDTDI, a modified scheme called S-FDTDII is then presented by reducing the perturbation error of S-FDTDI.

Consider the following two-dimensional transverse electric (TE) polarization case in a lossless medium as an example to demonstrate the theory of the splitting schemes:

$$\frac{\partial E_x}{\partial t} = \frac{1}{\varepsilon}\frac{\partial H_z}{\partial y}, \tag{2.1}$$

$$\frac{\partial E_y}{\partial t} = -\frac{1}{\varepsilon}\frac{\partial H_z}{\partial x}, \tag{2.2}$$

$$\frac{\partial H_z}{\partial t} = \frac{1}{\mu}\left(\frac{\partial E_x}{\partial y} - \frac{\partial E_y}{\partial x}\right), \tag{2.3}$$

where ε and μ are the electric permittivity and magnetic permeability of the medium, respectively, and $\mathbf{E} = (E_x(x, y, t), E_y(x, y, t))$ and $H_z = H_z(x, y, t)$ for $(x, y) \in \Omega = [0, a] \times [0, b]$ and $t \in (0, T]$ denote the electric field and the magnetic field, respectively. The spatial domain $\Omega = [0, a] \times [0, b]$ is occupied by this medium and surrounded by perfect conductors. So the perfectly conducting boundary condition is satisfied on the boundary:

$$(\mathbf{E}, 0) \times (\vec{n}, 0) = 0 \quad \text{on } (0, T] \times \partial\Omega, \tag{2.4}$$

where $\partial\Omega$ denotes the boundary of Ω and $\vec{n}$ is the outward normal vector on $\partial\Omega$. The initial conditions are

$$\mathbf{E}(x, y, 0) = \mathbf{E}_0(x, y) = (E_{x0}(x, y), E_{y0}(x, y)) \quad \text{and} \quad H_z(x, y, 0) = H_{z0}(x, y). \tag{2.5}$$

It is well known that, for suitably smooth data, problem (2.1)–(2.5) has a unique solution for all time (see [9]). For theoretical analysis, we will assume throughout this paper that the solution of the Maxwell system (2.1)–(2.5) has the following regularity property:

$$\begin{aligned} &\mathbf{E} \in C((0, T]; [C^3(\bar{\Omega})]^2) \cap C^1([0, T]; [C^1(\bar{\Omega})]^2) \cap C^2([0, T]; [C(\bar{\Omega})]^2), \\ &H_z \in C((0, T]; C^3(\bar{\Omega})) \cap C^1([0, T]; C^1(\bar{\Omega})) \cap C^2([0, T]; C(\bar{\Omega})). \end{aligned} \tag{2.6}$$

For simplicity in notations, we only consider the case of constant coefficients. The methods described here can be extended easily to the case of variable coefficients.

Let the partition of space domain Ω and time interval $[0, T]$ be an uniformly staggered grid as

$$x_i = i\Delta x, \quad x_{i+\frac{1}{2}} = x_i + \tfrac{1}{2}\Delta x, \quad i = 0, 1 \ldots, I-1, \quad x_I = I\Delta x = a,$$

$$y_j = j\Delta y, \quad y_{j+\frac{1}{2}} = (j + \tfrac{1}{2})\Delta y, \quad j = 0, 1, \ldots, J-1, \quad y_J = J\Delta y = b,$$

$$t^n = n\Delta t, \quad t^{n+\frac{1}{2}} = t^n + \tfrac{1}{2}\Delta t, \quad n = 0, 1, \ldots, N-1, \quad t^N = N\Delta t = T,$$

where Δx and Δy are the mesh sizes along the x and y directions, respectively, Δt is the time step size, and I and J are two integers. For a function $F(t, x, y)$, we further define

$$F^m_{\alpha,\beta} = F(m\Delta t, \alpha\Delta x, \beta\Delta y), \quad \delta_t F^m_{\alpha,\beta} = \frac{F^{m+\frac{1}{2}}_{\alpha,\beta} - F^{m-\frac{1}{2}}_{\alpha,\beta}}{\Delta t},$$

$$\delta_x F^m_{\alpha,\beta} = \frac{F^m_{\alpha+\frac{1}{2},\beta} - F^m_{\alpha-\frac{1}{2},\beta}}{\Delta x}, \quad \delta_y F^m_{\alpha,\beta} = \frac{F^m_{\alpha,\beta+\frac{1}{2}} - F^m_{\alpha,\beta-\frac{1}{2}}}{\Delta y},$$

$$\delta_u \delta_v F^m_{\alpha,\beta} = \delta_u(\delta_v F^m_{\alpha,\beta}), \quad u, v = x, y.$$

Denote by $E_v{}^m_{\alpha,\beta}$ and $H_z{}^m_{\alpha,\beta}$ the approximation of the electric field $E_v(t^m, x_\alpha, y_\beta)$ with $v = x, y$ and the magnetic field $H_z(t^m, x_\alpha, y_\beta)$, respectively. The splitting FDTD scheme (called S-FDTDI) for the Maxwell equations (2.1)–(2.5) is defined by two stages, which is based on a splitting of Maxwell's equations. To see this clearly, we split the

Maxwell equations (2.1)–(2.3) into the following form:

$$\frac{\partial E_x}{\partial t} = \frac{1}{\varepsilon}\frac{\partial H_z}{\partial y},$$
$$\frac{1}{2}\frac{\partial H_z}{\partial t} = \frac{1}{\mu}\frac{\partial E_x}{\partial y} \tag{2.7}$$

and

$$\frac{\partial E_y}{\partial t} = -\frac{1}{\varepsilon}\frac{\partial H_z}{\partial x},$$
$$\frac{1}{2}\frac{\partial H_z}{\partial t} = -\frac{1}{\mu}\frac{\partial E_y}{\partial x}. \tag{2.8}$$

Applying the spatial discretization approximation to Eqs. (2.7) and (2.8) we can get the S-FDTDI scheme.

Stage 1:

$$\frac{{E_y}_{i,j+\frac{1}{2}}^{n+1} - {E_y}_{i,j+\frac{1}{2}}^{n}}{\Delta t} = -\frac{1}{2\varepsilon}\,\delta_x\{{H_z}_{i,j+\frac{1}{2}}^{*} + {H_z}_{i,j+\frac{1}{2}}^{n}\},$$
$$\frac{{H_z}_{i+\frac{1}{2},j+\frac{1}{2}}^{*} - {H_z}_{i+\frac{1}{2},j+\frac{1}{2}}^{n}}{\Delta t} = -\frac{1}{2\mu}\,\delta_x\{{E_y}_{i+\frac{1}{2},j+\frac{1}{2}}^{n+1} + {E_y}_{i+\frac{1}{2},j+\frac{1}{2}}^{n}\}. \tag{2.9}$$

Stage 2:

$$\frac{{E_x}_{i+\frac{1}{2},j}^{n+1} - {E_x}_{i+\frac{1}{2},j}^{n}}{\Delta t} = \frac{1}{2\varepsilon}\,\delta_y\{{H_z}_{i+\frac{1}{2},j}^{n+1} + {H_y}_{i+\frac{1}{2},j}^{n}\},$$
$$\frac{{H_z}_{i+\frac{1}{2},j+\frac{1}{2}}^{n+1} - {H_z}_{i+\frac{1}{2},j+\frac{1}{2}}^{*}}{\Delta t} = \frac{1}{2\mu}\,\delta_y\{{E_x}_{i+\frac{1}{2},j+\frac{1}{2}}^{n+1} + {E_x}_{i+\frac{1}{2},j+\frac{1}{2}}^{n}\}. \tag{2.10}$$

By the definition of the cross product of vectors and the boundary condition (2.4), the boundary values for scheme (2.9)–(2.10) can be derived as follows:

$${E_x}_{i+\frac{1}{2},0}^{m} = {E_x}_{i+\frac{1}{2},J}^{m} = {E_y}_{0,j+\frac{1}{2}}^{m} = {E_y}_{I,j+\frac{1}{2}}^{m} = 0, \tag{2.11}$$

where $m = n$ or $m = n+1$ denotes any time level. Finally, the initial values $\mathbf{E}_{\alpha,\beta}^{0}$ and ${H_z}_{\alpha,\beta}^{0}$ are easily given as

$${E_x}_{\alpha,\beta}^{0} = E_{x0}(\alpha\Delta x, \beta\Delta y), \quad {E_y}_{\alpha,\beta}^{0} = E_{y0}(\alpha\Delta x, \beta\Delta y), \quad {H_z}_{\alpha,\beta}^{0} = H_{z0}(\alpha\Delta x, \beta\Delta y). \tag{2.12}$$

It can be seen from Eqs. (2.9)–(2.10) that the S-FDTDI scheme is very simple. Each stage, which contains only two equations, can be written equivalently as a tridiagonal system of linear equations for the electric field vector E_y^{n+1} (or E_x^{n+1}) and a direct formulation of obtaining the magnetic field vector H_z^* (or H_z^{n+1}) explicitly. For example, rewriting the second equation in (2.9) as

$${H_z}_{i+\frac{1}{2},j+\frac{1}{2}}^{*} = {H_z}_{i+\frac{1}{2},j+\frac{1}{2}}^{n} - \frac{\Delta t}{2\mu}\,\delta_x({E_y}_{i+\frac{1}{2},j+\frac{1}{2}}^{n+1} + {E_y}_{i+\frac{1}{2},j+\frac{1}{2}}^{n}), \tag{2.13}$$

and then substituting ${H_z}_{i+\frac{1}{2},j+\frac{1}{2}}^{*}$ into the first equation in (2.9) give a system of linear equations:

$$-\frac{(\Delta t)^2}{4\mu\varepsilon(\Delta x)^2}\,{E_y}_{i-1,j+\frac{1}{2}}^{n+1} + \left[1 + \frac{(\Delta t)^2}{2\mu\varepsilon(\Delta x)^2}\right]{E_y}_{i,j+\frac{1}{2}}^{n+1} - \frac{(\Delta t)^2}{4\mu\varepsilon(\Delta x)^2}\,{E_y}_{i+1,j+\frac{1}{2}}^{n+1}$$
$$= {E_y}_{i,j+\frac{1}{2}}^{n} - \frac{\Delta t}{\varepsilon}\,\delta_x {H_z}_{i,j+\frac{1}{2}}^{n} + \frac{(\Delta t)^2}{4\mu\varepsilon}\,\delta_x(\delta_x {E_y}_{i,j+\frac{1}{2}}^{n}). \tag{2.14}$$

System (2.14) is a tridiagonal system with a constant coefficient matrix (or a varying coefficient matrix on spatial index i, j when ε and μ are functions of x and y on domain Ω), which does not change for all time level n. All the field components on the right-hand side (RHS) have been obtained at the previous time step. So the system can be solved efficiently. Then, the corresponding $H_{z}^{*}{}_{i+1/2,j+1/2}$, $i=0,1,\ldots,I-1$, $j=0,1,\ldots,J-1$, can be obtained explicitly from formula (2.13).

Similarly, combining the two equations in (2.10), we can get another tridiagonal system of equations

$$-\frac{(\Delta t)^2}{4\mu\varepsilon(\Delta y)^2}E_x{}_{i+\frac{1}{2},j-1}^{n+1}+\left[1+\frac{(\Delta t)^2}{2\mu\varepsilon(\Delta y)^2}\right]E_x{}_{i+\frac{1}{2},j}^{n+1}-\frac{(\Delta t)^2}{4\mu\varepsilon(\Delta y)^2}E_x{}_{i+\frac{1}{2},j+1}^{n+1}$$
$$=E_x{}_{i+\frac{1}{2},j}^{n}+\frac{\Delta t}{\varepsilon}\delta_y(H_z{}_{i+\frac{1}{2},j}^{*}+H_z{}_{i+\frac{1}{2},j}^{n})+\frac{(\Delta t)^2}{4\mu\varepsilon}\delta_y(\delta_y E_x{}_{i+\frac{1}{2},j}^{n})$$

and

$$H_z{}_{i+\frac{1}{2},j+\frac{1}{2}}^{n+1}=H_z{}_{i+\frac{1}{2},j+\frac{1}{2}}^{*}+\frac{\Delta t}{2\mu}\delta_y\{E_x{}_{i+\frac{1}{2},j+\frac{1}{2}}^{n+1}+E_x{}_{i+\frac{1}{2},j+\frac{1}{2}}^{n}\}.$$

Remark 2.1. The S-FDTDI scheme is different from the conventional ADI procedure (see [12,4,2,1]), where the stages in the ADI schemes are made with respect to the two spatial coordinate directions or two terms containing derivatives along coordinate directions.

Remark 2.2. The S-FDTDI is also different from the 2D-ADI-FDTD scheme proposed in [10]. From (2.7) and (2.8) as well as (2.13) and (2.15), it can be seen that the values of the magnetic field at the intermediate time levels are not the real values of the magnetic field at that time levels. Furthermore, the S-FDTDI scheme contains only H_z^* but the 2D-ADI-FDTD scheme contains two more involved terms: $E_x^{n+\frac{1}{2}}$ and $E_y^{n+\frac{1}{2}}$ which are the real value of the electric fields at the intermediate time levels. At each stage, the S-FDTDI scheme contains only two equations, but the 2D-ADI-FDTD scheme consists of three equations. This simplicity of the S-FDTDI scheme makes it much more convenient to implement in practical computation.

The truncation error of the S-FDTDI scheme is of first order in time, as seen from the detailed analysis given in the next section using (3.3)–(3.5). To improve the accuracy of the S-FDTDI scheme, we propose a modified scheme by reducing the perturbation error of the S-FDTDI scheme. The modified scheme becomes a second-order perturbation to the CN scheme.

The modified splitting finite-difference time-domain scheme (called S-FDTDII) for the problem is given as follows.

Stage 1:

$$\frac{E_y{}_{i,j+\frac{1}{2}}^{n+1}-E_y{}_{i,j+\frac{1}{2}}^{n}}{\Delta t}=-\frac{1}{2\varepsilon}\delta_x\{H_z{}_{i,j+\frac{1}{2}}^{*}+H_z{}_{i,j+\frac{1}{2}}^{n}\}-\frac{\Delta t}{2\mu\varepsilon}\delta_x\delta_y E_x{}_{i,j+\frac{1}{2}}^{n},$$
$$\frac{H_z{}_{i+\frac{1}{2},j+\frac{1}{2}}^{*}-H_z{}_{i+\frac{1}{2},j+\frac{1}{2}}^{n}}{\Delta t}=-\frac{1}{2\mu}\delta_x\{E_y{}_{i+\frac{1}{2},j+\frac{1}{2}}^{n+1}+E_y{}_{i+\frac{1}{2},j+\frac{1}{2}}^{n}\}. \tag{2.15}$$

Stage 2:

$$\frac{E_x{}_{i+\frac{1}{2},j}^{n+1}-E_x{}_{i+\frac{1}{2},j}^{n}}{\Delta t}=\frac{1}{2\varepsilon}\delta_y\{H_z{}_{i+\frac{1}{2},j}^{n+1}+H_y{}_{i+\frac{1}{2},j}^{n}\},$$
$$\frac{H_z{}_{i+\frac{1}{2},j+\frac{1}{2}}^{n+1}-H_z{}_{i+\frac{1}{2},j+\frac{1}{2}}^{*}}{\Delta t}=\frac{1}{2\mu}\delta_y\{E_x{}_{i+\frac{1}{2},j+\frac{1}{2}}^{n+1}+E_x{}_{i+\frac{1}{2},j+\frac{1}{2}}^{n}\}. \tag{2.16}$$

The initial and boundary conditions for this scheme are the same as given for the S-FDTDI scheme.

The S-FDTDII (2.15)–(2.16) is just a modification of the S-FDTDI (2.9)–(2.10) by adding only one previous time level term into (2.9). The S-FDTDII scheme can also be solved easily in a similar way to solve the S-FDTDI scheme discussed above.

Remark 2.3. The truncation error of the S-FDTDII scheme is of second order in both space and time. To analyze the truncation error of the scheme, we derive an equivalent form of the S-FDTDII scheme by eliminating the magnetic field at the intermediate time level, H_z^* from the S-FDTDII Scheme (2.15)–(2.16):

$$\frac{E_x{}^{n+1}_{i+\frac{1}{2},j} - E_x{}^{n}_{i+\frac{1}{2},j}}{\Delta t} = \frac{1}{2\varepsilon}\,\delta_y(H_z{}^{n+1}_{i+\frac{1}{2},j} + H_z{}^{n}_{i+\frac{1}{2},j}), \tag{2.17}$$

$$\frac{E_y{}^{n+1}_{i,j+\frac{1}{2}} - E_y{}^{n}_{i,j+\frac{1}{2}}}{\Delta t} = -\frac{1}{2\varepsilon}\,\delta_x(H_z{}^{n+1}_{i,j+\frac{1}{2}} + H_z{}^{n}_{i,j+\frac{1}{2}}) + \frac{\Delta t}{4\mu\varepsilon}\,\delta_x\delta_y(E_x{}^{n+1}_{i,j+\frac{1}{2}} - E_x{}^{n}_{i,j+\frac{1}{2}}), \tag{2.18}$$

$$\frac{H_z{}^{n+1}_{i+\frac{1}{2},j+\frac{1}{2}} - H_z{}^{n}_{i+\frac{1}{2},j+\frac{1}{2}}}{\Delta t} = \frac{1}{2\mu}\{\delta_y(E_x{}^{n+1}_{i+\frac{1}{2},j+\frac{1}{2}} + E_x{}^{n}_{i+\frac{1}{2},j+\frac{1}{2}}) - \delta_x(E_y{}^{n+1}_{i+\frac{1}{2},j+\frac{1}{2}} + E_y{}^{n}_{i+\frac{1}{2},j+\frac{1}{2}})\}. \tag{2.19}$$

Scheme (2.17)–(2.19) is the CN scheme for the Maxwell equations plus a second-order perturbation term (the last term of Eq. (2.18)). Thus, the S-FDTDII scheme is equivalent to a second-order perturbation of the CN scheme, so the truncation error of the scheme is of second order in both space and time.

Remark 2.4. The S-FDTDII scheme is also different from the 2D-ADI-FDTD scheme proposed in [10]. The S-FDTDII scheme, which contains only two equations at each stage, is much simpler in the final algebraic system and easier in programming compared with the 2D-ADI-FDTD scheme. This will save computational work and CPU time (see numerical experiments in Section 5). On the other hand, the S-FDTDII scheme is different from the S-FDTDI scheme only by one term in the first equation at stage 1. This added term contains only one previous time level values, which is different from that in [3], where a term containing two time levels is added to the ADI scheme for a parabolic equation.

Remark 2.5. Our technique of deriving the improved splitting scheme, S-FDTDII, is based on an idea introduced by Douglas and Kim in [3] for the ADI scheme of parabolic equations. A different procedure to improve the truncation error of splitting schemes is Strang's splitting: a half-step in one direction, a whole step in the other, a half-step in the first direction. However, this splitting technique of Strang is not straightforward for the S-FDTDI scheme and needs further study.

3. Stability and convergence analysis

In this section, we consider the stability and convergence of the S-FDTDI scheme, employing the energy method. For grid functions $U := \{U_{i+1/2,j}, i = 0, 1, \ldots, I-1,\ j = 1, 2, \ldots, J-1\}$, $V := \{V_{i,j+1/2}, i = 1, \ldots, I-1,\ j = 0, 1, \ldots, J-1\}$, $W := \{W_{i+1/2,j+1/2}, i = 0, 1, \ldots, I-1,\ j = 0, 1, \ldots, J-1\}$ and $\mathbf{F} := \{(U_{i+1/2,j}, V_{i,j+1/2}), i = 0, 1, \ldots, I-1,\ j = 1, 2, \ldots, J-1\}$, we introduce the following norms:

$$\|U\|^2_{E_x} = \sum_{i=0}^{I-1}\sum_{j=1}^{J-1}(U_{i+\frac{1}{2},j})^2\Delta x\Delta y, \quad \|V\|^2_{E_y} = \sum_{i=1}^{I-1}\sum_{j=0}^{J-1}(V_{i,j+\frac{1}{2}})^2\Delta x\Delta y,$$

$$\|W\|^2_{H_z} = \sum_{i=0}^{I-1}\sum_{j=0}^{J-1}(W_{i+\frac{1}{2},j+\frac{1}{2}})^2\Delta x\Delta y, \quad \|\mathbf{F}\|^2_E = \|U\|^2_{E_x} + \|V\|^2_{E_y}.$$

Then the main results on stability and convergence of the S-FDTDI scheme are expressed as follows.

Theorem 3.1. *Suppose that the exact solution components E_x, E_y and H_z satisfy the regularity property* (2.6). *For $n \geqslant 0$, let*

$$\mathbf{E}^n := \{(E_x{}^n_{i+\frac{1}{2},j}, E_y{}^n_{i,j+\frac{1}{2}}),\ i = 0, 1, \ldots, I-1,\ j = 1, 2, \ldots, J-1\},$$

$$H_z^{n+1} := \{H_z{}^n_{i+\frac{1}{2},j+\frac{1}{2}},\ i = 0, 1, \ldots, I-1,\ j = 1, 2, \ldots, J-1\}$$

be the solution of the S-FDTDI scheme (2.9)–(2.10). *Then, for any fixed $T > 0$ there is a positive constant C independent of Δt, Δx and Δy such that*

$$\max_{0\leqslant n\leqslant N}\{\|\varepsilon^{\frac{1}{2}}[\mathbf{E}(t^n) - \mathbf{E}^n]\|_E + \|\mu^{\frac{1}{2}}[H_z(t^n) - H_z^n]\|_{H_z}\} \leqslant C[\Delta t + (\Delta x)^2 + (\Delta y)^2], \tag{3.1}$$

$$\max_{0\leqslant n\leqslant N}\{\|\varepsilon^{\frac{1}{2}}\delta_t[\mathbf{E}(t^{n+\frac{1}{2}}) - \mathbf{E}^{n+\frac{1}{2}}]\|_E + \|\mu^{\frac{1}{2}}\delta_t\,[H_z(t^{n+\frac{1}{2}}) - H_z^{n+\frac{1}{2}}]\|_{H_z}\} \leqslant C[\Delta t + (\Delta x)^2 + (\Delta y)^2]. \tag{3.2}$$

Proof. From the second equation of (2.10), we can get the expression of $H_{z\,i+1/2,j+1/2}^{*}$. Then substituting it into the first equation of (2.9), we obtain the following form of the scheme:

$$\frac{E_x{}^{n+1}_{i+\frac{1}{2},j} - E_x{}^n_{i+\frac{1}{2},j}}{\Delta t} = \frac{1}{2\varepsilon}\,\delta_y(H_z{}^{n+1}_{i+\frac{1}{2},j} + H_z{}^n_{i+\frac{1}{2},j}), \tag{3.3}$$

$$\frac{E_y{}^{n+1}_{i,j+\frac{1}{2}} - E_y{}^n_{i,j+\frac{1}{2}}}{\Delta t} = -\frac{1}{2\varepsilon}\,\delta_x(H_z{}^{n+1}_{i,j+\frac{1}{2}} + H_z{}^n_{i,j+\frac{1}{2}}) + \frac{\Delta t}{4\mu\varepsilon}\,\delta_x\delta_y\{E_x{}^{n+1}_{i,j+\frac{1}{2}} + E_x{}^n_{i,j+\frac{1}{2}}\}, \tag{3.4}$$

$$\frac{H_z{}^{n+1}_{i+\frac{1}{2},j+\frac{1}{2}} - H_z{}^n_{i+\frac{1}{2},j+\frac{1}{2}}}{\Delta t} = \frac{1}{2\mu}\,\{\delta_y(E_x{}^{n+1}_{i+\frac{1}{2},j+\frac{1}{2}} + E_x{}^n_{i+\frac{1}{2},j+\frac{1}{2}}) - \delta_x(E_y{}^{n+1}_{i+\frac{1}{2},j+\frac{1}{2}} + E_y{}^n_{i+\frac{1}{2},j+\frac{1}{2}})\}. \tag{3.5}$$

From (3.3)–(3.5), it is easy to see that the scheme is equivalent to a first-order perturbation of the CN scheme for the Maxwell equations in two dimensions. Thus, the corresponding truncation errors are of first order in time where the perturbation error dominates the truncation error.

Let

$$\mathscr{E}_w{}^n_{\alpha,\beta} = E_w(t^n, x_\alpha, y_\beta) - E_w{}^n_{\alpha,\beta}, \quad \mathscr{H}_z{}^n_{\alpha,\beta} = H_z(t^n, x_\alpha, y_\beta) - H_z{}^n_{\alpha,\beta},$$

where $E_w(t^n, x_\alpha, y_\beta)$ with $w = x, y$ and $H_z(t^n, x_\alpha, y_\beta)$ denote the values of the exact solution components E_w with $w = x, y$ and H_z at the point (t^n, x_α, y_β), and all the subscripts α, β take their valid choices. Set $\mathscr{E}^n = (\mathscr{E}_x^n, \mathscr{E}_y^n)$. Subtracting (3.3)–(3.5) from (2.1)–(2.3), we obtain the following error equations:

$$\frac{\mathscr{E}_x{}^{n+1}_{i+\frac{1}{2},j} - \mathscr{E}_x{}^n_{i+\frac{1}{2},j}}{\Delta t} = \frac{1}{2\varepsilon}\,\delta_y(\mathscr{H}_z{}^{n+1}_{i+\frac{1}{2},j} + \mathscr{H}_z{}^n_{i+\frac{1}{2},j}) + \xi_x{}^{n+\frac{1}{2}}_{i+\frac{1}{2},j}, \tag{3.6}$$

$$\frac{\mathscr{E}_y{}^{n+1}_{i,j+\frac{1}{2}} - \mathscr{E}_y{}^n_{i,j+\frac{1}{2}}}{\Delta t} = -\frac{1}{2\varepsilon}\,\delta_x(\mathscr{H}_z{}^{n+1}_{i,j+\frac{1}{2}} + \mathscr{H}_z{}^n_{i,j+\frac{1}{2}}) + \frac{\Delta t}{4\mu\varepsilon}\,\delta_x\delta_y(\mathscr{E}_x{}^{n+1}_{i,j+\frac{1}{2}} + \mathscr{E}_x{}^n_{i,j+\frac{1}{2}}) + \xi_y{}^{n+\frac{1}{2}}_{i,j+\frac{1}{2}}, \tag{3.7}$$

$$\begin{aligned}\frac{\mathscr{H}_z{}^{n+1}_{i+\frac{1}{2},j+\frac{1}{2}} - \mathscr{H}_z{}^n_{i+\frac{1}{2},j+\frac{1}{2}}}{\Delta t} &= \frac{1}{2\mu}\{\delta_y(\mathscr{E}_x{}^{n+1}_{i+\frac{1}{2},j+\frac{1}{2}} + \mathscr{E}_x{}^n_{i+\frac{1}{2},j+\frac{1}{2}}) - \delta_x(\mathscr{E}_y{}^{n+1}_{i+\frac{1}{2},j+\frac{1}{2}} + \mathscr{E}_y{}^n_{i+\frac{1}{2},j+\frac{1}{2}})\}\\ &\quad + \eta_z{}^{n+\frac{1}{2}}_{i+\frac{1}{2},j+\frac{1}{2}},\end{aligned} \tag{3.8}$$

where $\xi_w^{n+\frac{1}{2}}$ with $w = x, y$ and $\eta_z^{n+\frac{1}{2}}$ are the truncation errors which can be written as

$$\xi_{x\,i+\frac{1}{2},j}^{n+\frac{1}{2}} = (\Delta t)^2\left[\frac{1}{24}\frac{\partial^3 E_x}{\partial t^3}(\tau_{11}, x_{i+\frac{1}{2}}, y_j) + \frac{1}{8\varepsilon}\frac{\partial^3 H_z}{\partial t^2 \partial y}(\tau_{12}, x_{i+\frac{1}{2}}, y_{11})\right] + \frac{(\Delta y)^2}{24\varepsilon}\frac{\partial^3 H_z}{\partial y^3}(t^{n+\frac{1}{2}}, x_{i+\frac{1}{2}}, y_{12}),$$

$$\xi_{y\,i,j+\frac{1}{2}}^{n+\frac{1}{2}} = \frac{\Delta t}{4\mu\varepsilon}\frac{\partial^2 E_x}{\partial x \partial y}(\tau_{21}, x_{21}, y_{21}) - (\Delta t)^2\left[\frac{1}{24}\frac{\partial^3 E_y}{\partial t^3}(\tau_{22}, x_i, y_{j+\frac{1}{2}}) - \frac{1}{8\varepsilon}\frac{\partial^3 H_z}{\partial t^2 \partial x}(\tau_{23}, x_{22}, y_{j+\frac{1}{2}})\right]$$
$$- \frac{(\Delta x)^2}{24\varepsilon}\frac{\partial^3 H_z}{\partial x^3}(t^{n+\frac{1}{2}}, x_{23}, y_{j+\frac{1}{2}}),$$

$$\eta_{z\,i+\frac{1}{2},j+\frac{1}{2}}^{n+\frac{1}{2}} = (\Delta t)^2\left[-\frac{1}{24}\frac{\partial^3 H_z}{\partial t^3}(\tau_{31}, x_{i+\frac{1}{2}}, y_{j+\frac{1}{2}}) + \frac{1}{8\mu}\frac{\partial^3 E_x}{\partial t^2 \partial y}(\tau_{32}, x_{i+\frac{1}{2}}, y_{31}) - \frac{1}{8\mu}\frac{\partial^3 E_y}{\partial t^2 \partial x}(\tau_{33}, x_{31}, y_{j+\frac{1}{2}})\right]$$
$$+ \frac{1}{24\mu}\left[(\Delta y)^2\frac{\partial^3 E_x}{\partial y^3}(t^{n+\frac{1}{2}}, x_{i+\frac{1}{2}}, y_{32}) + (\Delta x)^2\frac{\partial^3 E_y}{\partial x^3}(t^{n+\frac{1}{2}}, x_{32}, y_{j+\frac{1}{2}})\right],$$

where $t^n \leqslant \tau_{1l},\ \tau_{2k},\ \tau_{3k} \leqslant t^{n+1}$, $x_{i-\frac{1}{2}} \leqslant x_{2k}, x_{3l} \leqslant x_{i+\frac{1}{2}}$, $y_{j-\frac{1}{2}} \leqslant y_{1l}, y_{21}, y_{3l} \leqslant y_{j+\frac{1}{2}}$ with $l = 1, 2$ and $k = 1, 2, 3$. Thus, it holds that

$$|\xi_{x\,i+\frac{1}{2},j,k}^{n+\frac{1}{2}}| \leqslant (\Delta t)^2\left(\frac{1}{24}\left\|\frac{\partial^3 E_x}{\partial t^3}\right\|_\infty + \frac{1}{8\varepsilon}\left\|\frac{\partial^3 H_z}{\partial y \partial t^2}\right\|_\infty\right) + \frac{(\Delta y)^2}{24\varepsilon}\left\|\frac{\partial^3 H_z}{\partial y^3}\right\|_\infty$$
$$\leqslant C_{\mu\varepsilon} M\{(\Delta t)^2 + (\Delta y)^2\},$$

$$|\xi_y^{n+\frac{1}{2}}| \leqslant C_{\mu\varepsilon} M\{\Delta t + (\Delta t)^2 + (\Delta x)^2\},$$

$$|\eta_z^{n+\frac{1}{2}}| \leqslant C_{\mu\varepsilon} M\{(\Delta t)^2 + (\Delta x)^2 + (\Delta y)^2\},$$

where $C_{\mu\varepsilon}$ and M are two constants:

$$C_{\mu\varepsilon} = [1/24 + 1/(8\varepsilon) + 1/(8\mu)],$$

$$M = \max\{\|\partial_t^3 F\|_\infty, \|\partial_u^3 H_z\|_\infty, \|\partial_u^3 E_v\|_\infty, \|\partial_u \partial_t^2 H_z\|_\infty,$$
$$\|\partial_u \partial_t^2 E_v\|_\infty, \|\partial_x \partial_y E_x\|_\infty | F = E_x,\ E_y,\ H_z, u, v = x, y, u \neq v\}.$$

Multiplying both sides of (3.6) with $\sqrt{\varepsilon}\Delta t$, regrouping terms so that the terms with the time index of $n+1$ are on the left-hand side (LHS) and the others on the RHS, and then squaring both sides of the equation thus obtained, we obtain that

$$\varepsilon(\mathscr{E}_{x\,i+\frac{1}{2},j}^{n+1})^2 + \frac{(\Delta t)^2}{4\varepsilon}(\delta_y \mathscr{H}_{z\,i+\frac{1}{2},j}^{n+1})^2 - \Delta t\,\mathscr{E}_{x\,i+\frac{1}{2},j}^{n+1} \cdot \delta_y \mathscr{H}_{z\,i+\frac{1}{2},j}^{n+1}$$
$$\leqslant (1 + \Delta t)\left\{\varepsilon(\mathscr{E}_{x\,i+\frac{1}{2},j}^{n})^2 + \frac{(\Delta t)^2}{4\varepsilon}(\delta_y \mathscr{H}_{z\,i+\frac{1}{2},j}^{n})^2 + \Delta t\,\mathscr{E}_x^n \cdot \delta_y \mathscr{H}_{z\,i+\frac{1}{2},j}^{n} + \varepsilon\Delta t(\xi_{x\,i+\frac{1}{2},j}^{n+\frac{1}{2}})^2\right\}, \tag{3.9}$$

where use has been made of the inequality $(a+\Delta t b)^2 \leqslant (1+\Delta t)(a^2+b^2)$. Multiplying (3.9) with $\Delta x \Delta y$ and summing up over i, j from $i = 0, 1, \ldots, I-1$, $j = 1, 2, \ldots, J-1$, we then have

$$\begin{aligned}
&\sum_{i=0}^{I-1}\sum_{j=1}^{J-1}\left[\varepsilon(\mathscr{E}_x{}_{i+\frac{1}{2},j}^{n+1})^2+\frac{(\Delta t)^2}{4\varepsilon}(\delta_y\mathscr{H}_z{}_{i+\frac{1}{2},j}^{n+1})^2-\Delta t\mathscr{E}_x{}_{i+\frac{1}{2},j}^{n+1}\cdot\delta_y\mathscr{H}_z{}_{i+\frac{1}{2},j}^{n+1}\right]\Delta x\Delta y\\
&\leqslant\sum_{i=0}^{I-1}\sum_{j=1}^{J-1}\left[(1+\Delta t)\left\{\varepsilon(\mathscr{E}_x{}_{i+\frac{1}{2},j}^{n})^2+\frac{(\Delta t)^2}{4\varepsilon}(\delta_y\mathscr{H}_z{}_{i+\frac{1}{2},j}^{n})^2+\Delta t\mathscr{E}_x^n\cdot\delta_y\mathscr{H}_z{}_{i+\frac{1}{2},j}^{n}\right.\right.\\
&\quad\left.\left.+\varepsilon\Delta t(\xi_x{}_{i+\frac{1}{2},j}^{n+\frac{1}{2}})^2\right\}\right]\Delta x\Delta y. \qquad (3.10)
\end{aligned}$$

A similar procedure can be applied to the other two Eqs. (3.7) and (3.8) and the corresponding two inequalities similar to (3.10) can be obtained. Adding these inequalities together gives the following relation:

$$\begin{aligned}
&\sum_{i=0}^{I-1}\sum_{j=1}^{J-1}\left[\varepsilon(\mathscr{E}_x{}_{i+\frac{1}{2},j}^{n+1})^2+\frac{(\Delta t)^2}{4\varepsilon}(\delta_y\mathscr{H}_z{}_{i+\frac{1}{2},j}^{n+1})^2-\Delta t\mathscr{E}_x{}_{i+\frac{1}{2},j}^{n+1}\cdot\delta_y\mathscr{H}_z{}_{i+\frac{1}{2},j}^{n+1}\right]\Delta x\Delta y+\sum_{i=1}^{I-1}\sum_{j=0}^{J-1}\left[\varepsilon(\mathscr{E}_y{}_{i,j+\frac{1}{2}}^{n+1})^2\right.\\
&+\frac{(\Delta t)^2}{4\varepsilon}\left(\delta_x\mathscr{H}_z{}_{i,j+\frac{1}{2}}^{n+1}-\frac{\Delta t}{2\mu}\delta_x\delta_y\mathscr{E}_x{}_{i,j+\frac{1}{2}}^{n+1}\right)^2+\Delta t\mathscr{E}_y{}_{i,j+\frac{1}{2}}^{n+1}\cdot\delta_x\mathscr{H}_z{}_{i,j+\frac{1}{2}}^{n+1}\\
&\left.-\frac{(\Delta t)^2}{2\mu}\delta_x\delta_y\mathscr{E}_x{}_{i,j+\frac{1}{2}}^{n+1}\cdot\mathscr{E}_y{}_{i,j+\frac{1}{2}}^{n+1}\right]\Delta x\Delta y+\sum_{i=0}^{I-1}\sum_{j=0}^{J-1}\left[\mu(\mathscr{H}_z{}_{i+\frac{1}{2},j+\frac{1}{2}}^{n+1})^2\right.\\
&+\frac{(\Delta t)^2}{4\mu}(\delta_x\mathscr{E}_y{}_{i+\frac{1}{2},j+\frac{1}{2}}^{n+1})^2+\frac{(\Delta t)^2}{4\mu}(\delta_y\mathscr{E}_x{}_{i+\frac{1}{2},j+\frac{1}{2}}^{n+1})^2-\Delta t\mathscr{H}_z{}_{i+\frac{1}{2},j+\frac{1}{2}}^{n+1}\cdot\delta_y\mathscr{E}_x{}_{i+\frac{1}{2},j+\frac{1}{2}}^{n+1}\\
&\left.+\Delta t\mathscr{H}_z{}_{i+\frac{1}{2},j+\frac{1}{2}}^{n+1}\cdot\delta_x\mathscr{E}_y{}_{i+\frac{1}{2},j+\frac{1}{2}}^{n+1}-\frac{(\Delta t)^2}{2\mu}\delta_y\mathscr{E}_x{}_{i+\frac{1}{2},j+\frac{1}{2}}^{n+1}\cdot\delta_x\mathscr{E}_y{}_{i+\frac{1}{2},j+\frac{1}{2}}^{n+1}\right]\Delta x\Delta y\\
&\leqslant(1+\Delta t)\left\{\sum_{i=0}^{I-1}\sum_{j=1}^{J-1}\left[\varepsilon(\mathscr{E}_x{}_{i+\frac{1}{2},j}^{n})^2+\frac{(\Delta t)^2}{4\varepsilon}(\delta_y\mathscr{H}_z{}_{i+\frac{1}{2},j}^{n})^2+\Delta t\mathscr{E}_x{}_{i+\frac{1}{2},j}^{n}\cdot\delta_y\mathscr{H}_z{}_{i+\frac{1}{2},j}^{n}\right.\right.\\
&\quad\left.+\varepsilon\Delta t(\xi_x{}_{i+\frac{1}{2},j}^{n+\frac{1}{2}})^2\right]\Delta x\Delta y+\sum_{i=1}^{I-1}\sum_{j=0}^{J-1}\left[\varepsilon(\mathscr{E}_y{}_{i,j+\frac{1}{2}}^{n})^2+\frac{(\Delta t)^2}{4\varepsilon}\left(\delta_x\mathscr{H}_z{}_{i,j+\frac{1}{2}}^{n}-\frac{\Delta t}{2\mu}\delta_x\delta_y\mathscr{E}_x{}_{i,j+\frac{1}{2}}^{n}\right)^2\right.\\
&\quad\left.-\Delta t\mathscr{E}_y{}_{i,j+\frac{1}{2}}^{n}\cdot\delta_x\mathscr{H}_z{}_{i,j+\frac{1}{2}}^{n}+\frac{(\Delta t)^2}{2\mu}\mathscr{E}_y{}_{i,j+\frac{1}{2}}^{n}\cdot\delta_x\delta_y\mathscr{E}_x{}_{i,j+\frac{1}{2}}^{n}+\varepsilon\Delta t(\xi_y{}_{i,j+\frac{1}{2}}^{n+\frac{1}{2}})^2\right]\Delta x\Delta y\\
&\quad+\sum_{i=0}^{I-1}\sum_{j=0}^{J-1}\left[\mu(\mathscr{H}_z{}_{i+\frac{1}{2},j+\frac{1}{2}}^{n})^2+\frac{(\Delta t)^2}{4\mu}(\delta_x\mathscr{E}_y{}_{i+\frac{1}{2},j+\frac{1}{2}}^{n})^2+\frac{(\Delta t)^2}{4\mu}(\delta_y\mathscr{E}_x{}_{i+\frac{1}{2},j+\frac{1}{2}}^{n})^2\right.\\
&\quad+\Delta t\mathscr{H}_z{}_{i+\frac{1}{2},j+\frac{1}{2}}^{n}\cdot\delta_y\mathscr{E}_x{}_{i+\frac{1}{2},j+\frac{1}{2}}^{n}-\Delta t\mathscr{H}_z{}_{i+\frac{1}{2},j+\frac{1}{2}}^{n}\cdot\delta_x\mathscr{E}_y{}_{i+\frac{1}{2},j+\frac{1}{2}}^{n}\\
&\quad\left.\left.-\frac{(\Delta t)^2}{2\mu}\delta_y\mathscr{E}_x{}_{i+\frac{1}{2},j+\frac{1}{2}}^{n}\cdot\delta_x\mathscr{E}_y{}_{i+\frac{1}{2},j+\frac{1}{2}}^{n}+\mu\Delta t(\eta_z{}_{i+\frac{1}{2},j+\frac{1}{2}}^{n+\frac{1}{2}})^2\right]\Delta x\Delta y\right\}. \qquad (3.11)
\end{aligned}$$

The sums of all mixed-product terms on the LHS and RHS of (3.11) can be canceled out with each other by using summation by parts and the boundary conditions (2.11). For example, consider the mixed-product terms on the LHS

of (3.11). The first mixed-product term in the third "$\sum\sum$" sign of the LHS of (3.11) can be written as

$$
\begin{aligned}
-\sum_{i=0}^{I-1}\sum_{j=0}^{J-1}\Delta t\,\mathscr{H}_z{}_{i+\frac{1}{2},j+\frac{1}{2}}^{n+1}\cdot\delta_y\mathscr{E}_x{}_{i+\frac{1}{2},j+\frac{1}{2}}^{n+1} &= -\sum_{i=0}^{I-1}\frac{\Delta t}{\Delta y}\left[\mathscr{H}_z{}_{i+\frac{1}{2},J-\frac{1}{2}}^{n+1}\cdot\mathscr{E}_x{}_{i+\frac{1}{2},J}^{n+1}-\mathscr{H}_z{}_{i+\frac{1}{2},\frac{1}{2}}^{n+1}\cdot\mathscr{E}_x{}_{i+\frac{1}{2},0}^{n+1}\right.\\
&\quad\left.-\sum_{j=1}^{J-1}\mathscr{E}_x{}_{i+\frac{1}{2},j}^{n+1}\cdot(\mathscr{H}_z{}_{i+\frac{1}{2},j+\frac{1}{2}}^{n+1}-\mathscr{H}_z{}_{i+\frac{1}{2},j-\frac{1}{2}}^{n+1})\right]\\
&= \sum_{i=0}^{I-1}\sum_{j=1}^{J-1}\Delta t\,\mathscr{E}_x{}_{i+\frac{1}{2},j}^{n+1}\cdot\delta_y\mathscr{H}_z{}_{i+\frac{1}{2},j}^{n+1},
\end{aligned}
\tag{3.12}
$$

where use has been made of the boundary conditions (2.11) so that

$$
\mathscr{E}_x{}_{i+\frac{1}{2},0}^{n+\frac{1}{2}}=\mathscr{E}_x{}_{i+\frac{1}{2}J}^{n+\frac{1}{2}}=0,\quad i=0,1,\ldots,I-1.
$$

We can see that the RHS of (3.12) is canceled out by the third mixed-product term on the LHS of (3.11). Similarly, we can prove that the second mixed-product term on the third "$\sum\sum$" sign of the LHS of (3.11) can be canceled out by the sixth term. Consider now the last term on the LHS of (3.11), which is

$$
\begin{aligned}
-\sum_{i=0}^{I-1}\sum_{j=0}^{J-1}\frac{(\Delta t)^2}{2\mu}\delta_y\mathscr{E}_x{}_{i+\frac{1}{2},j+\frac{1}{2}}^{n+1}\cdot\delta_x\mathscr{E}_y{}_{i+\frac{1}{2},j+\frac{1}{2}}^{n+1} &= -\sum_{j=0}^{J-1}\frac{(\Delta t)^2}{2\mu\Delta x}[\mathscr{E}_y{}_{I,j+\frac{1}{2}}^{n+1}\cdot\delta_y\mathscr{E}_x{}_{I-\frac{1}{2},j+\frac{1}{2}}^{n+1}\\
&\quad-\mathscr{E}_y{}_{0,j+\frac{1}{2}}^{n+1}\cdot\delta_y\mathscr{E}_x{}_{\frac{1}{2},j+\frac{1}{2}}^{n+1}]\\
&\quad+\sum_{i=1}^{I-1}\sum_{j=0}^{J-1}\frac{(\Delta t)^2}{2\mu}\mathscr{E}_y{}_{i,j+\frac{1}{2}}^{n+1}\cdot\delta_x\delta_y\mathscr{E}_x{}_{i,j+\frac{1}{2}}^{n+1}\\
&= \sum_{i=1}^{I-1}\sum_{j=0}^{J-1}\frac{(\Delta t)^2}{2\mu}\mathscr{E}_y{}_{i,j+\frac{1}{2}}^{n+1}\cdot\delta_x\delta_y\mathscr{E}_x{}_{i,j+\frac{1}{2}}^{n+1}.
\end{aligned}
$$

This plus the seventh term on the LHS of (3.11) is equal to zero. Thus, all the mixed-product terms on the LHS of (3.11) can be canceled out by each other. The same argument can be used in canceling out the mixed-product terms on the RHS of (3.11). Thus, we finally have that

$$
\begin{aligned}
&\|\varepsilon^{\frac{1}{2}}\boldsymbol{\mathscr{E}}^{n+1}\|_E^2+\|\mu^{\frac{1}{2}}\mathscr{H}_z^{n+1}\|_H^2+\frac{(\Delta t)^2}{4}\left\|\varepsilon^{-\frac{1}{2}}\left(\delta_x\mathscr{H}_z^{n+1}-\frac{\Delta t}{2\mu}\delta_x\delta_y\mathscr{E}_x^{n+1}\right)\right\|_{E_y}^2\\
&\quad+\frac{(\Delta t)^2}{4}(\|\varepsilon^{-\frac{1}{2}}\delta_y\mathscr{H}_z^{n+1}\|_{E_x}^2+\|\mu^{-\frac{1}{2}}\delta_x\mathscr{E}_y^{n+1}\|_H^2+\|\mu^{-\frac{1}{2}}\delta_y\mathscr{E}_x^{n+1}\|_H^2)\\
&\quad\leqslant(1+\Delta t)\left\{\|\varepsilon^{\frac{1}{2}}\mathscr{E}^n\|_E^2+\|\mu^{\frac{1}{2}}\mathscr{H}_z^n\|_H^2+\frac{(\Delta t)^2}{4}\left\|\varepsilon^{-\frac{1}{2}}(\delta_x\mathscr{H}_z^n-\frac{\Delta t}{2\mu}\delta_x\delta_y\mathscr{E}_x^n)\right\|_{E_y}^2\right.\\
&\qquad\left.+\frac{(\Delta t)^2}{4}(\|\varepsilon^{-\frac{1}{2}}\delta_y\mathscr{H}_z^n\|_{E_x}^2+\|\mu^{-\frac{1}{2}}\delta_x\mathscr{E}_y^n\|_H^2+\|\mu^{-\frac{1}{2}}\delta_y\mathscr{E}_x^n\|_H^2)+\Delta t(\|\varepsilon^{\frac{1}{2}}\boldsymbol{\xi}^{n+\frac{1}{2}}\|_E^2+\|\mu^{\frac{1}{2}}\eta_z^{n+\frac{1}{2}}\|_H^2)\right\},
\end{aligned}
$$

where $\boldsymbol{\xi}^{n+\frac{1}{2}}=(\xi_x^{n+\frac{1}{2}},\xi_y^{n+\frac{1}{2}})$. This inequality together with the estimates of truncation errors implies estimate (3.1).

To prove (3.2), subtract each of Eqs. (3.6)–(3.8) with n replaced by $n-1$ from itself to get three new error equations. Then estimate (3.2) can be derived by a similar argument as above. This ends the proof. □

Similarly, we have the following stability theorem.

Theorem 3.2. *Let $n \geqslant 0$ and let*

$$\mathbf{E}^n := \{(E_x{}^n_{i+\frac{1}{2},j}, E_y{}^n_{i,j+\frac{1}{2}}),\ i=0,1,\ldots,I-1,\ j=1,2,\ldots,J-1\},$$

$$H_z^{n+1} := \{H_z{}^n_{i+\frac{1}{2},j+\frac{1}{2}},\ i=0,1,\ldots,I-1,\ j=1,2,\ldots,J-1\}$$

be the solution of the S-FDTDI scheme (2.9)–(2.10). *Then it holds that*

$$\begin{aligned}
&\|\varepsilon^{\frac{1}{2}}\mathbf{E}^{n+1}\|_E^2 + \|\mu^{\frac{1}{2}}H_z^{n+1}\|_{H_z}^2 + \frac{(\Delta t)^2}{4\varepsilon}\left\|\delta_x H_z^{n+1} - \frac{\Delta t}{2\mu}\delta_x\delta_y E_x^{n+1}\right\|_{E_y}^2 \\
&\quad + \frac{(\Delta t)^2}{4}(\|\varepsilon^{-\frac{1}{2}}\delta_y H_z^{n+1}\|_{E_x}^2 + \|\mu^{-\frac{1}{2}}\delta_x E_y^{n+1}\|_{H_z}^2 + \|\mu^{-\frac{1}{2}}\delta_y E_x^{n+1}\|_{H_z}^2) \\
&\quad \leqslant \|\varepsilon^{\frac{1}{2}}\mathbf{E}^0\|_E^2 + \|\mu^{\frac{1}{2}}H_z^0\|_{H_z}^2 + \frac{(\Delta t)^2}{4\varepsilon}\left\|\delta_x H_z^0 - \frac{\Delta t}{2\mu}\delta_x\delta_y E_x^0\right\|_{E_y}^2 \\
&\qquad + \frac{(\Delta t)^2}{4}(\|\varepsilon^{-\frac{1}{2}}\delta_y H_z^0\|_{E_x}^2 + \|\mu^{-\frac{1}{2}}\delta_x E_y^0\|_{H_z}^2 + \|\mu^{-\frac{1}{2}}\delta_y E_x^0\|_{H_z}^2), \\
&\|\varepsilon^{\frac{1}{2}}\delta_t\mathbf{E}^{n+\frac{1}{2}}\|_E^2 + \|\mu^{\frac{1}{2}}\delta_t H_z^{n+\frac{1}{2}}\|_{H_z}^2 + \frac{(\Delta t)^2}{4\varepsilon}\left\|\delta_t\delta_x H_z^{n+\frac{1}{2}} - \frac{\Delta t}{2\mu}\delta_t\delta_x\delta_y E_x^{n+\frac{1}{2}}\right\|_{E_y}^2 \\
&\quad + \frac{(\Delta t)^2}{4}(\|\varepsilon^{-\frac{1}{2}}\delta_t\delta_y H_z^{n+\frac{1}{2}}\|_{E_x}^2 + \|\mu^{-\frac{1}{2}}\delta_t\delta_x E_y^{n+\frac{1}{2}}\|_{H_z}^2 + \|\mu^{-\frac{1}{2}}\delta_t\delta_y E_x^{n+\frac{1}{2}}\|_{H_z}^2) \\
&\quad \leqslant \|\varepsilon^{\frac{1}{2}}\delta_t\mathbf{E}^{\frac{1}{2}}\|_E^2 + \|\mu^{\frac{1}{2}}\delta_t H_z^{\frac{1}{2}}\|_{H_z}^2 + \frac{(\Delta t)^2}{4\varepsilon}\left\|\delta_t\delta_x H_z^{\frac{1}{2}} - \frac{\Delta t}{2\mu}\delta_t\delta_x\delta_y E_x^{\frac{1}{2}}\right\|_{E_y}^2 \\
&\qquad + \frac{(\Delta t)^2}{4}(\|\varepsilon^{-\frac{1}{2}}\delta_t\delta_y H_z^{\frac{1}{2}}\|_{E_x}^2 + \|\mu^{-\frac{1}{2}}\delta_t\delta_x E_y^{\frac{1}{2}}\|_{H_z}^2 + \|\mu^{-\frac{1}{2}}\delta_t\delta_y E_x^{\frac{1}{2}}\|_{H_z}^2).
\end{aligned}$$

Thus, the S-FDTDI scheme is unconditionally stable.

4. Numerical dispersion analysis

In this section we study the dispersion and dissipation properties of the S-FDTDI and S-FDTDII schemes using a Fourier analysis. The results show that the S-FDTDI scheme is unconditionally stable and dissipative and that the S-FDTDII scheme is unconditionally stable and non-dissipative.

4.1. Dispersion and dissipation properties

Let the trial time-harmonic solution of the Maxwell equations be

$$\mathbf{E}^n_{\alpha,\beta} = \mathbf{E_0}\xi^n \mathrm{e}^{-\mathrm{i}(k_x\alpha\Delta x + k_y\beta\Delta y)}, \quad H_z{}^n_{\alpha,\beta} = H_{z0}\xi^n \mathrm{e}^{-\mathrm{i}(k_x\alpha\Delta x + k_y\beta\Delta y)},$$

where $\mathrm{i}=\sqrt{-1}$ is the complex number, $\mathbf{E_0}=(E_{x0},\ E_{y0})^{\tau}$, k_x and k_y are the wavenumbers along the x-axis and y-axis, ξ is the stability factor. Substituting $\mathbf{E}^n_{\alpha,\beta}$ and $H_{z\alpha,\beta}^n$ into Eqs. (2.17)–(2.19) and eliminating the common factors yield

$$(\xi-1)E_{x0}+\mathrm{i}\,\frac{\Delta t}{\varepsilon}(\xi+1)b_yH_{z0}=0,$$

$$(\xi-1)E_{y0}+\frac{(\Delta t)^2}{\mu\varepsilon}(\xi-1)b_ya_xE_{x0}-\mathrm{i}\,\frac{\Delta t}{\varepsilon}(\xi+1)a_xH_{z0}=0,$$

$$\mathrm{i}\,\frac{\Delta t}{\mu}(\xi+1)b_yE_{x0}-\mathrm{i}\,\frac{\Delta t}{\mu}(\xi+1)a_xE_{y0}+(\xi-1)H_{z0}=0,$$

where

$$a_x=\sin^2(\tfrac{1}{2}k_x\Delta x)/(\Delta x)^2,\quad b_y=\sin^2(\tfrac{1}{2}k_y\Delta y)/(\Delta y)^2.$$

Noting that the unknowns $(E_{x0},\ E_{y0},\ H_{z0})$ of this algebraic system is a non-zero vector, the determinant of the coefficient matrix should be zero. Evaluating the third-order determinant and collecting the like terms, we get the equation of the stability factor ξ for the S-FDTDII scheme:

$$(\xi-1)(d_0\xi^2+2d_1\xi+d_0)^2=0, \tag{4.1}$$

where

$$d_0=1+\frac{(\Delta t)^2}{\mu\varepsilon}[(a_x)^2+(b_y)^2]+\frac{(\Delta t)^4}{(\mu\varepsilon)^2}(a_xb_y)^2,$$

$$d_1=-1+\frac{(\Delta t)^2}{\mu\varepsilon}[(a_x)^2+(b_y)^2]+\frac{(\Delta t)^4}{(\mu\varepsilon)^2}(a_xb_y)^2.$$

The roots of Eq. (4.1) is easy to work out, which are

$$\xi_1=1,\quad \xi_2=(d_0)^{-1}\left(-d_1+\mathrm{i}\sqrt{d_0^2-d_1^2}\right),\quad \xi_3=(d_0)^{-1}\left(-d_1-\mathrm{i}\sqrt{d_0^2-d_1^2}\right).$$

Clearly, the modulus of these three roots is equal to one, which means that the S-FDTDII scheme is unconditional stable and non-dissipative.

For the S-FDTDI scheme, the equation of the stability factor ξ can be obtained similarly:

$$c_3\xi^3+c_2\xi^2+c_1\xi+c_0=0, \tag{4.2}$$

where

$$c_3=1+\frac{(\Delta t)^2}{\mu\varepsilon}[(a_x)^2+(b_y)^2]+\frac{(\Delta t)^4}{(\mu\varepsilon)^2}(a_xb_y)^2,$$

$$c_2=-3+\frac{(\Delta t)^2}{\mu\varepsilon}[(a_x)^2+(b_y)^2]+3\,\frac{(\Delta t)^4}{(\mu\varepsilon)^2}(a_xb_y)^2,$$

$$c_1=3-\frac{(\Delta t)^2}{\mu\varepsilon}(a_x^2+b_y^2)+3\,\frac{(\Delta t)^4}{(\mu\varepsilon)^2}(a_xb_y)^2,$$

$$c_0=-1-\frac{(\Delta t)^2}{\mu\varepsilon}[(a_x)^2+(b_y)^2]+\frac{(\Delta t)^4}{(\mu\varepsilon)^2}(a_xb_y)^2.$$

Note that

$$k_x=k\cos(\phi),\quad k_y=k\sin(\phi),\quad k^2=(k_x)^2+(k_y)^2,\quad N_\lambda=\frac{\lambda}{h},\quad \omega=ck, \tag{4.3}$$

where k and ϕ are the spherical coordinates of the wavenumber vector $\mathbf{K}$, λ is the wavelength, $\Delta x=\Delta y=h$ is the spatial step size, and N_λ is the number of points per wavelength (NPPW). Let $S=c\Delta t/h$ be the CFL number (in fact,

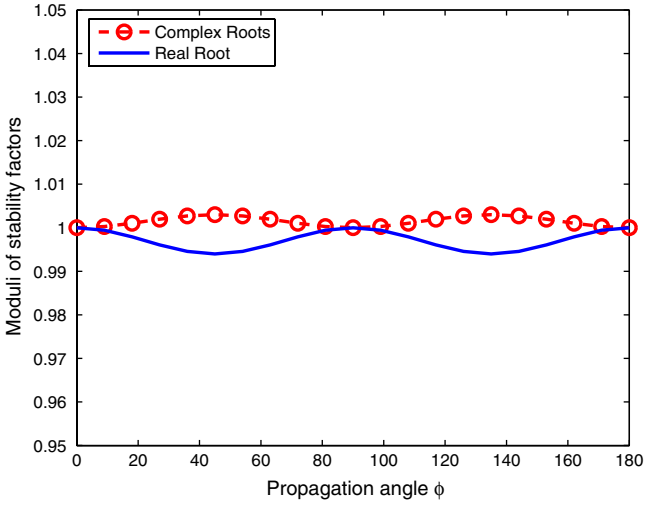

Fig. 1. Modulus of stability factor of S-FDTDI against propagation angle with $S = 1.4$.

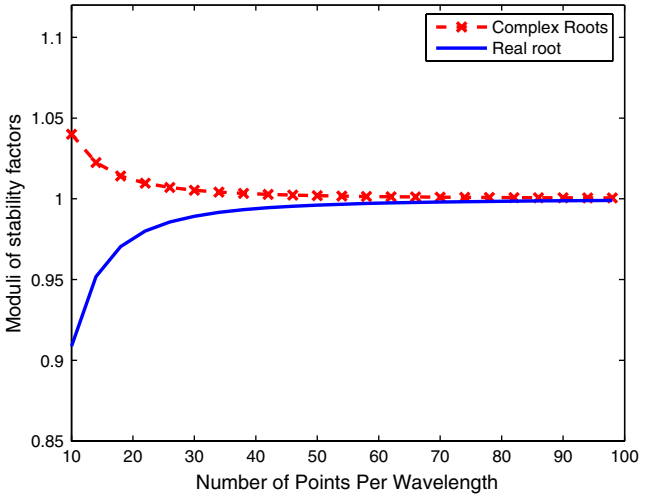

Fig. 2. Modulus of stability factor of S-FDTDI against NPPW with $\phi = 35°$, $S = 1.5$.

the CFL number is $\sqrt{2}c\Delta t/h$). It is clear that the stability factor ξ is a function of S, ϕ and N_λ, that is, $\xi = \xi(S, \phi, N_\lambda)$. Figs. 1–3 show the approximation results of the stability factor ξ of the S-FDTDI scheme.

Fig. 1 shows the variation of the modulus $|\xi|$ of the three roots of Eq. (4.2) against ϕ with $S = 1.4$ and $N_\lambda = 40$, where the lower curve corresponds to the real root while the upper curve corresponds to the two complex roots (the curves corresponding to the two complex roots coincide with each other). It can be seen that the modulus of the principal roots (the complex roots) is bigger than 1 but $|\xi| = 1 + \mathrm{O}(\Delta t)$. Since $\Delta t = S \times 1/N_\lambda = 1.4 \times 1/40 = 0.035$, it is clear that the curves are between the two straight lines: $y = 1 \pm 0.035$, which corresponds to the result that the S-FDTDI scheme is unconditionally stable in the energy norm (since $(1 + \Delta t)^n \leqslant \mathrm{e}^T$ for all $n > 0$). This also implies that the S-FDTDI scheme is dissipative.

Figs. 2 and 3 give the variation of the modulus $|\xi|$ against the number of points per wavelength with $\phi = 35°$ and $S = 1.5$, and against the CFL number S with $N_\lambda = 60$ and $\phi = 65°$, respectively. Similarly to the analysis above for Fig. 1, it can be seen clearly that the S-FDTDI scheme is unconditional stable and dissipative.

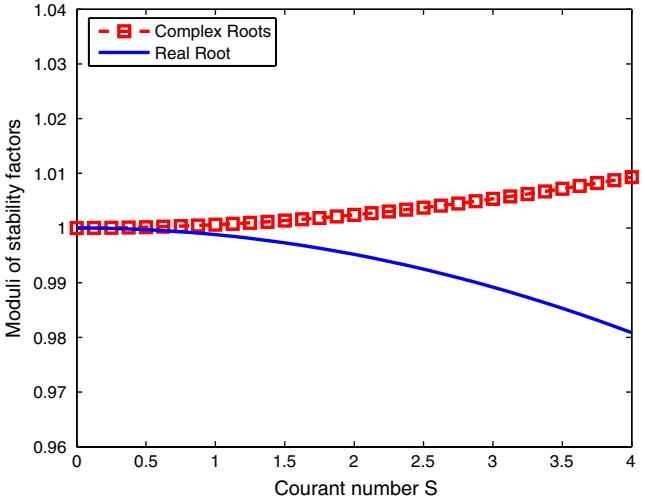

Fig. 3. Modulus of the stability factor of S-FDTDI against S with $N_\lambda = 60$, $\phi = 35°$.

Remark 4.1. The equation of the stability factor of the CN scheme for the two-dimensional Maxwell equations is

$$(\xi - 1)(\bar{d}_0\xi^2 + 2\bar{d}_1\xi + \bar{d}_0)^2 = 0, \tag{4.4}$$

where

$$\bar{d}_0 = 1 + \frac{(\Delta t)^2}{\mu\varepsilon}[(a_x)^2 + (b_y)^2],$$

$$\bar{d}_1 = -1 + \frac{(\Delta t)^2}{\mu\varepsilon}[(a_x)^2 + (b_y)^2].$$

The modulus $|\xi|$ of the roots of (4.4) is 1, which means that the CN scheme is unconditionally stable and non-dissipative.

4.2. Numerical dispersion relations

Let the trial time-harmonic solution of the Maxwell equations be

$$\mathbf{E}^n_{\alpha,\beta} = \mathbf{E_0}\mathrm{e}^{\mathrm{i}(k_x\alpha\Delta x + k_y\beta\Delta y - \omega n\Delta t)}, \quad H_z{}^n_{\alpha,\beta} = H_{z0}\mathrm{e}^{\mathrm{i}(k_x\alpha\Delta x + k_y\beta\Delta y - \omega n\Delta t)}, \tag{4.5}$$

where $\mathbf{E}_0$ is a complex vector, H_{z0} is a complex number, k_x and k_y are the wavenumber along the x-axis and y-axis, respectively. Then, substituting $\mathbf{E}^n_{\alpha,\beta}$ and $H_z{}^n_{\alpha,\beta}$ into the equivalent form of the S-FDTDII scheme (see (2.17)–(2.19)) and eliminating the common factors yield that

$$\sin(\tfrac{1}{2}\omega\Delta t)E_{x0} + (\Delta t/\varepsilon)\cos(\tfrac{1}{2}\omega\Delta t)b_y H_{z0} = 0,$$

$$\sin(\tfrac{1}{2}\omega\Delta t)E_{y0} + (c\Delta t)^2\sin(\tfrac{1}{2}\omega\Delta t)b_y a_x E_{x0} - (\Delta t/\varepsilon)\cos(\tfrac{1}{2}\omega\Delta t)a_x H_{z0} = 0,$$

$$(\Delta t/\mu)\cos(\tfrac{1}{2}\omega\Delta t)b_y E_{x0} - (\Delta t/\mu)\cos(\tfrac{1}{2}\omega\Delta t)a_x E_{y0} + \sin(\tfrac{1}{2}\omega\Delta t)H_{z0} = 0.$$

Since the unknowns (E_{x0}, E_{y0}, H_{z0}) of this algebraic system is non-zero, then the determinant of the coefficient matrix should be zero. By collecting the like terms and factoring the equation thus obtained, we get the numerical dispersion

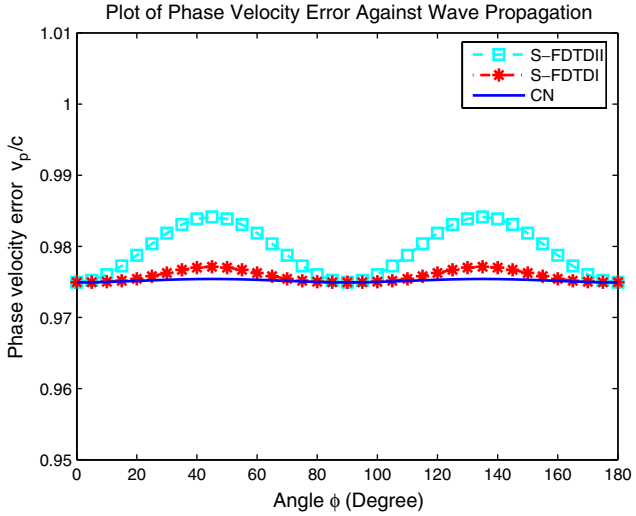

Fig. 4. Numerical phase velocity of the three schemes (S-FDTDI, S-FDTDII, CN) against the angle ϕ with $S = 3.5$ and $N_\lambda = 40$.

relation of the S-FDTDII scheme:

$$\sin^2\left(\frac{1}{2}\omega\Delta t\right) = (c\Delta t)^2 \cdot \left[\frac{\sin^2(\frac{1}{2}k_x\Delta x)}{(\Delta x)^2} + \frac{\sin^2(\frac{1}{2}k_y\Delta y)}{(\Delta y)^2}\right] \cdot \cos^2\left(\frac{1}{2}\omega\Delta t\right) + (c\Delta t)^4 \cdot \frac{\sin^2(\frac{1}{2}k_x\Delta x)}{(\Delta x)^2} \cdot \frac{\sin^2(\frac{1}{2}k_y\Delta y)}{(\Delta y)^2} \cdot \cos^2\left(\frac{1}{2}\omega\Delta t\right), \tag{4.6}$$

where $c^2 = 1/(\mu\varepsilon)$.

Similarly, we get the numerical dispersion relation of the S-FDTDI scheme:

$$\sin^2\left(\frac{1}{2}\omega\Delta t\right) = (c\Delta t)^2 \cdot \left[\frac{\sin^2(\frac{1}{2}k_x\Delta x)}{(\Delta x)^2} + \frac{\sin^2(\frac{1}{2}k_y\Delta y)}{(\Delta y)^2}\right] \cdot \cos^2\left(\frac{1}{2}\omega\Delta t\right) + (c\Delta t)^4 \frac{\sin^2(\frac{1}{2}k_x\Delta x)}{(\Delta x)^2} \cdot \frac{\sin^2(\frac{1}{2}k_y\Delta y)}{(\Delta y)^2} \cos^3\left(\frac{1}{2}\omega\Delta t\right) \sin^{-1}\left(\frac{1}{2}\omega\Delta t\right), \tag{4.7}$$

and the numerical dispersion relation of the CN scheme:

$$\sin^2\left(\frac{1}{2}\omega\Delta t\right) = (c\Delta t)^2 \cdot \left[\frac{\sin^2(\frac{1}{2}k_x\Delta x)}{(\Delta x)^2} + \frac{\sin^2(\frac{1}{2}k_y\Delta y)}{(\Delta y)^2}\right] \cdot \cos^2\left(\frac{1}{2}\omega\Delta t\right). \tag{4.8}$$

Noting that

$$\lim_{x\to 0}\frac{\sin(x)}{x} = 1, \quad \lim_{x\to 0}\cos(x) = 1,$$

it is easy to see that the numerical dispersion relations (4.1), (4.2) and (4.4) converge to the analytical dispersion relation of the problem:

$$\omega^2 = c^2[(k_x)^2 + (k_y)^2],$$

when the time step Δt and the spatial steps Δx, Δy tend to zero. Further, comparing these relations, it is seen that the numerical dispersion relations of the S-FDTDI scheme and the S-FDTDII scheme are first-order and second-order in time perturbations of the numerical dispersion relation of the CN scheme, respectively. This indicates that the dispersion error of the S-FDTDII scheme is smaller than that of the S-FDTDI scheme.

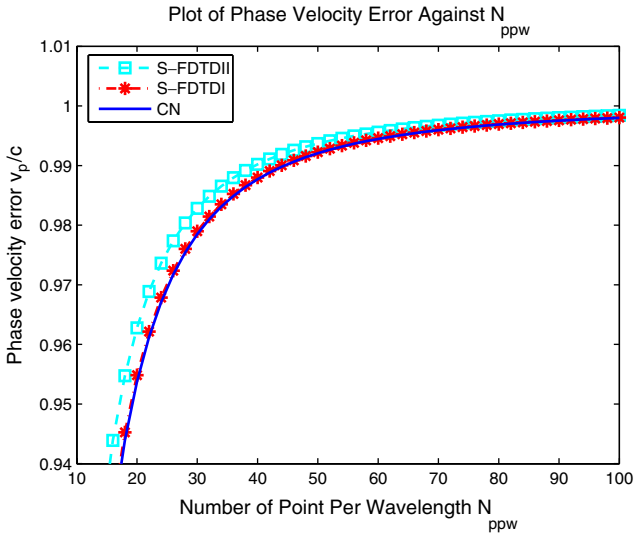

Fig. 5. Numerical phase velocity of the three schemes (S-FDTDI, S-FDTDII, CN) against the number N_λ of points per wavelength with $\phi = 65°$ and $S = 2.4$.

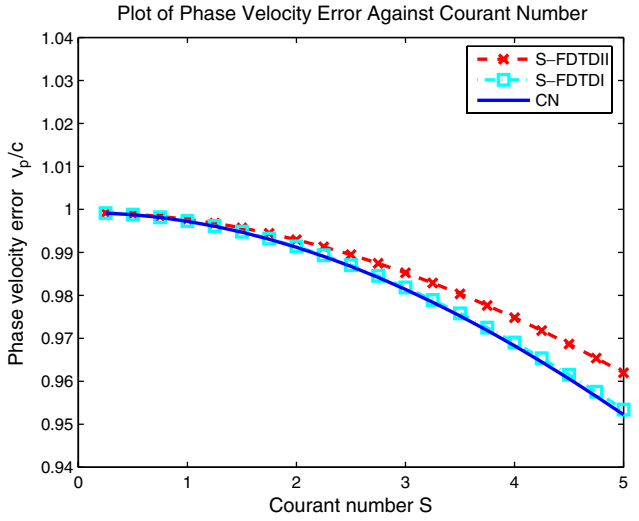

Fig. 6. Numerical phase velocity of the three schemes (S-FDTDI, S-FDTDII, CN) against the CFL number S with $\phi = 65°$ and $N_\lambda = 40$.

4.3. Numerical dispersion errors

We now present the numerical dispersion errors of the three schemes (the S-FDTDI scheme, the S-FDTDII scheme and the CN scheme) with different grid sizes, wave propagation angles and CFL numbers.

Let $\xi = e^{i\omega\Delta t}$, which is a root of Eqs. (4.1), (4.2) or (4.4). If ω is a complex number, $\omega = \omega_R + i\omega_I$, where ω_R and ω_I are the real and imaginary part, respectively, then $\xi = e^{-\omega_I\Delta t}[\cos(\omega_R\Delta t) + i\ \sin(\omega_R\Delta t)]$ and $\tan(\omega_R\Delta t)) = \Im(\xi)/\Re(\xi)$ with $\Im(\xi)$ and $\Re(\xi)$ denoting the imaginary and real parts of ξ, respectively. So, using the notations in (4.3) we can express the numerical phase velocity v_p normalized to the speed of light, c, as

$$\frac{v_p}{c} = \frac{\omega_R/k}{c} = \frac{1}{ck\Delta t}\arctan\left(\frac{\Im(\xi)}{\Re(\xi)}\right) = \frac{N_\lambda}{2\pi S}\arctan\left(\frac{\Im(\xi)}{\Re(\xi)}\right),$$

where S is the CFL number, N_λ is the number of points per wavelength, and k is the wavenumber (that is, the modulus of the wavenumber vector $\mathbf{K}$).

Figs. 4–6 compare the normalized phase velocity v_p/c of the S-FDTDI scheme, the S-FDTDII scheme and the CN scheme against ϕ, S and N_λ.

Fig. 4 gives the variation of the normalized phase velocity v_p/c against the wave propagation ϕ with $N_\lambda = 40$ and $S = 3.5$. It can be seen clearly that the ratio v_p/c of the S-FDTDII scheme is more close to 1 than that of the S-FDTDI and CN schemes, so the dispersion error of the S-FDTDII scheme is smaller than that of the S-FDTDI and CN schemes.

Figs. 5 and 6 show the variation of v_p/c against the number of points per wavelength, N_λ, with $\phi = 65^\circ$ and $S = 2.4$, and against the CFL number S with $\phi = 65^\circ$ and $N_\lambda = 40$, respectively. It is seen that the numerical dispersion errors become bigger when the CFL number becomes bigger or the number of points per wavelength becomes smaller. In these cases, the numerical dispersion error of the S-FDTDII scheme is much smaller than those of the S-FDTDI and CN schemes.

5. Numerical experiments

In this section we present numerical experiments of our S-FDTD schemes for solving the two-dimensional Maxwell equations with PEC boundary conditions and for solving a scattering problem with the perfectly matched sponger layers (see [19,13]). Numerical results by our S-FDTD schemes are compared with those by the 2D-ADI-FDTD scheme in [10] and the Yee scheme. Numerical Experiments show the effective performance of our S-FDTD schemes.

5.1. The Maxwell equations with PEC boundary conditions

In this experiment, we use the S-FDTDI and S-FDTDII schemes to solve the two-dimensional Maxwell equations with PEC boundary conditions.

Set the region $\Omega = [0, 1] \times [0, 1]$ surrounded by a perfect conductor and consider the Maxwell equations (2.1)–(2.5) in a lossless medium with normalized electric permittivity and magnetic permeability, that is, $\varepsilon = \mu = 1$. The exact solution of the problem is

$$E_x = \cos(\sqrt{2}\pi t)\cos[\pi(1-x)]\sin[\pi(1-y)],$$

$$E_y = -\cos(\sqrt{2}\pi t)\sin[\pi(1-x)]\cos[\pi(1-y)],$$

$$H_z = -\sqrt{2}\sin(\sqrt{2}\pi t)\cos[\pi(1-x)]\cos[\pi(1-y)].$$

The drive routines are written in Fortran 77, and the computation was run in a 1.70 GHz PC having 256 MB RAM and Windows 2000 operating system. The experiments are carried out with different mesh sizes. The elapsed CPU time: CPU (seconds), numerical errors of $\mathbf{E}$ and H_z (under the energy norm defined in Section 3): Err-E, Err-H, and the convergence rate: Ra-E and Ra-H, are shown in Tables 1–3.

Table 1 shows the numerical results by the three methods (S-FDTDI, S-FDTDII and 2D-ADI-FDTD) at time $t = 1$ with $\Delta x = \Delta y = h = 0.001$. Table 2 gives the numerical results by the S-FDTDII scheme and the 2D-ADI-FDTD scheme at time $t = 1$ where the spatial step size is $\Delta x = \Delta y = h = 5 \times 10^{-4}$. From Table 1, it is clearly seen that the numerical results obtained by the S-FDTDII scheme are much more accurate than those by the S-FDTDI scheme. This indicates that the technique of reducing the perturbation error is successful in improving the accuracy of the S-FDTDI scheme. From the rate of convergence in the time step size Δt in the table, it is clear that the S-FDTDI scheme is of first-order convergence and that the S-FDTDII scheme is of second-order convergence. Comparing the results by the S-FDTDII scheme with those by the 2D-ADI-FDTD scheme in both Tables 1 and 2, it can be found that the accuracies of the two schemes are the same but the S-FDTDII scheme takes much less CPU time than the 2D-ADI-FDTD scheme does. Table 3 shows the elapsed CPU time and the CPU time saved by the S-FDTDII scheme in the case with $h = 0.001$ and different time step sizes at a long time $T = 6$. From this table it is very clear that the S-FDTDII scheme can save more and more CPU time than the 2D-ADI-FDTD scheme does as time step size becomes smaller and smaller, up to 50% or more CPU time.

Table 1
Performance of S-FDTDI, S-FDTDII and ADI-FDTD with $h = 0.001$

Scheme	Δt	Err-E	Err-H	Ra-E	Ra-H	CPU
S-FDTDI	$2h$	1.318872803052034e−2	1.639369025611106e−2			0.33
	$1h$	6.194149166630896e−3	8.282944096857309e−3	1.09	0.99	0.63
	$\frac{h}{2}$	3.035343932143145e−3	4.147606328998647e−3	1.029	1.00	1.27
	$\frac{h}{4}$	1.538906680538937e−3	2.062136487904849e−3	0.98	1.01	2.55
S-FDTDII	$2h$	1.438186790009288e−3	5.474977753515592e−4			0.33
	$1h$	4.495161266478538e−4	1.625371789689091e−4	1.68	1.75	0.72
	$\frac{h}{2}$	2.042138236525231e−4	6.64321871839632e−5	1.14	1.29	1.36
	$\frac{h}{4}$	1.441441083167702e−4	4.241440436801956e−5	0.50	0.65	2.75
2D-ADI-FDTD	$2h$	1.438186790009284e−3	5.474977753515786e−4			0.48
	$1h$	4.495161266478422e−4	1.625371789688881e−4	1.68	1.75	0.89
	$\frac{h}{2}$	2.042138236525155e−4	6.643218718398982e−5	1.14	1.29	1.80
	$\frac{h}{4}$	1.441441083167673e−4	4.241440436794655e−5	0.50	0.65	3.52

Table 2
Performance of S-FDTDII and ADI-FDTD with $h = 0.50\text{e} - 3$

Scheme	Δt	Err-E	Err-H	Ra-E	Ra-H	CPU
S-FDTDII	$16h$	2.11687296690431e−4	8.20508301529716e−5			1021.78
	$10h$	8.28747463415610e−5	3.20988100468914e−5	1.995	1.997	1684.36
	$8h$	5.31463419883299e−5	2.05735025724781e−5	1.991	1.993	2033.95
	$5h$	2.09396472331106e−5	8.08863429669419e−6	1.982	1.986	3271
2D-ADI-FDTD	$16h$	2.11687296690911e−4	8.20508301540433e−5			1415.39
	$10h$	8.28747463415920e−5	3.20988100476860e−5	1.995	1.997	2340.72
	$8h$	5.31463419883153e−5	2.05735025724595e−5	1.991	1.993	2821.19
	$5h$	2.09396472345299e−5	8.08863429393404e−6	1.982	1.986	4557.34

Table 3
CPU time by S-FDTDII and ADI-FDTD with $h = 0.001$ and $\Delta t = h/2$ at $t = 6$

Scheme	Err-E	Err-H	CPU time
S-FDTDII	1.25845411097222e−5	6.91284231049606e−7	21485.44
2D-ADI-FDTD	1.25845411096653e−5	6.91284231709626e−7	30988.56

5.2. A scattering problem with PML boundary conditions

In this experiment, we consider the problem of scattering of a point source in the case with two dielectric materials in the trip $S = \{-1 \leqslant x \leqslant 1,\ -0.2 \leqslant y \leqslant 2.2\}$, where periodic boundary conditions are assumed at the sides $x = \pm 2$ and PML sponge layers [19,13] are placed in the upper $(2 \leqslant y \leqslant 2.2)$ and lower $(-0.2 \leqslant y \leqslant 0)$ parts of the domain with electric and magnetic losses (see [16]):

$$\sigma = 0, \quad 0 \leqslant y \leqslant 2,$$

$$\sigma = \sigma_m \left(\frac{y}{0.2}\right)^2, \quad -0.2 \leqslant y \leqslant 0,$$

$$\sigma = \sigma_m \left(\frac{y-2}{0.2}\right)^2, \quad 2 < y \leqslant 2.2.$$

We assume that perfectly conducting boundary conditions are satisfied at the end of the PML layers. We assume further that $\mu = 1$, $\sigma_m = 43.17$ and

$$\varepsilon = 1 \quad \text{for } 0 < y < 1,$$

$$\varepsilon = 4 \quad \text{for } 1 < y < 2.$$

With r being the distance from a point to (0, 0.5), the initial fields are defined by

$$E_x^0 = -(y - 0.5)H_z^0$$

$$E_y^0 = xH_z^0$$

$$H_z^0 = \frac{1}{36}\left(12 + 15\cos\left(\frac{10\pi r}{3}\right) + 6\cos\left(\frac{20\pi r}{3}\right) + 3\cos(10\pi r)\right) \quad \text{if } r \leqslant 0.3,$$

$$H_z^0 = 0 \quad \text{otherwise.}$$

This arrangement creates a radially symmetric pulse.

By the theory of PML sponge layers (see [19,13]), the Maxwell equations in the PML sponge layers can be written as

$$\frac{\partial E_x}{\partial t} + \sigma E_x = \frac{1}{\varepsilon}\frac{\partial H_z}{\partial y}, \tag{5.1}$$

$$\varepsilon\frac{\partial E_y}{\partial t} = -\frac{\partial H_z}{\partial x} - \sigma\int_0^t \frac{\partial H_z}{\partial x}\,\mathrm{d}t, \tag{5.2}$$

$$\frac{\partial H_z}{\partial t} + \sigma H_z = \frac{1}{\mu}\left(\frac{\partial E_x}{\partial y} - \frac{\partial E_y}{\partial x}\right). \tag{5.3}$$

The S-FDTDII scheme for the Maxwell equations (5.1)–(5.3) is given in the following two stages:

Stage 1:

$$\begin{aligned}\frac{{E_y}_{i,j+\frac{1}{2}}^{n+1} - {E_y}_{i,j+\frac{1}{2}}^{n}}{\Delta t} &= -\frac{1}{2\varepsilon}\delta_x\{{H_z}_{i,j+\frac{1}{2}}^{*} + {H_z}_{i,j+\frac{1}{2}}^{n}\} - \frac{\sigma_{j+\frac{1}{2}}}{\varepsilon}\left(\sum_{k=0}^{n-1}(\delta_x H_z^k + \delta_x H_z^{k+1})\frac{\Delta t}{2}\right.\\ &\quad \left. + (\delta_x H_z^n + \delta_x H_z^*)\frac{\Delta t}{4}\right) - \frac{\Delta t}{2\mu\varepsilon}\left(1 + \frac{\Delta t}{2}\sigma_{j+\frac{1}{2}}\right)\delta_x\delta_y {E_x}_{i,j+\frac{1}{2}}^{n}\\ &\quad \times \frac{{H_z}_{i+\frac{1}{2},j+\frac{1}{2}}^{*} - {H_z}_{i+\frac{1}{2},j+\frac{1}{2}}^{n}}{\Delta t} + \sigma_{j+\frac{1}{2}}\frac{{H_z}_{i+\frac{1}{2},j+\frac{1}{2}}^{*} + {H_z}_{i+\frac{1}{2},j+\frac{1}{2}}^{n}}{2}\\ &= -\frac{1}{2\mu}\delta_x\{{E_y}_{i+\frac{1}{2},j+\frac{1}{2}}^{n+1} + {E_y}_{i+\frac{1}{2},j+\frac{1}{2}}^{n}\} - \frac{\Delta t}{2\mu}\sigma_{j+\frac{1}{2}}\delta_y {E_x}_{i+\frac{1}{2},j+\frac{1}{2}}^{n}.\end{aligned}$$

Stage 2:

$$\frac{{E_x}_{i+\frac{1}{2},j}^{n+1} - {E_x}_{i+\frac{1}{2},j}^{n}}{\Delta t} + \sigma_j\frac{{E_x}_{i+\frac{1}{2},j}^{n+1} + {E_x}_{i+\frac{1}{2},j}^{n}}{2} = \frac{1}{2\varepsilon}\delta_y\{{H_z}_{i+\frac{1}{2},j}^{n+1} + {H_y}_{i+\frac{1}{2},j}^{n}\},$$

$$\frac{{H_z}_{i+\frac{1}{2},j+\frac{1}{2}}^{n+1} - {H_z}_{i+\frac{1}{2},j+\frac{1}{2}}^{*}}{\Delta t} = \frac{1}{2\mu}\delta_y\{{E_x}_{i+\frac{1}{2},j+\frac{1}{2}}^{n+1} + {E_x}_{i+\frac{1}{2},j+\frac{1}{2}}^{n}\}.$$

We take the grid step sizes $\Delta x = \Delta y = h = 0.01$. The numerical results obtained by the S-FDTDI scheme, the S-FDTDII scheme, the 2D-ADI-FDTD scheme and the Yee scheme are presented in Figs. 7–9.

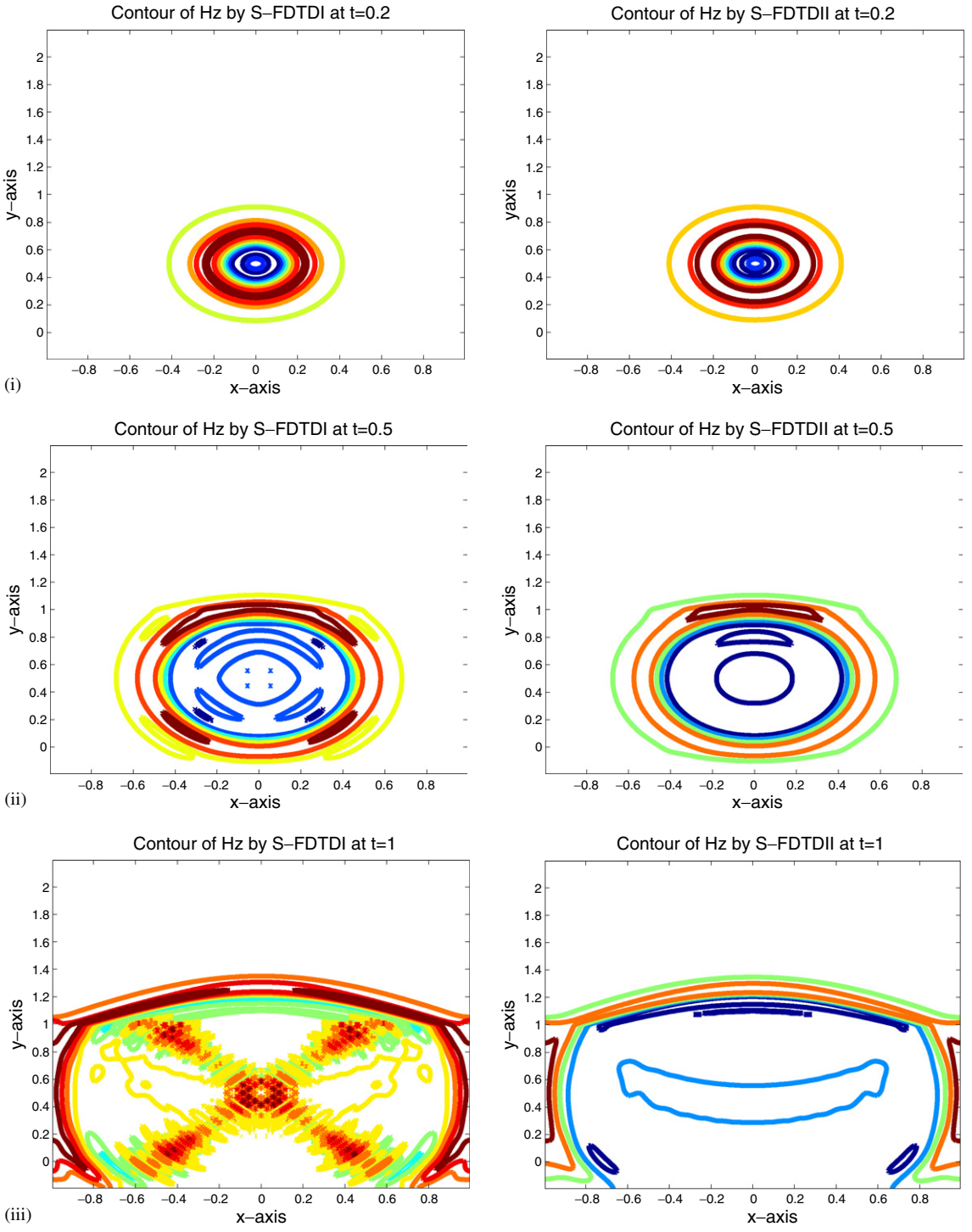

Fig. 7. Contour of H_z by S-FDTDI (left) and S-FDTDII (right) with $h = 0.01$ and $\Delta t = 2h$. (i) $t = 0.2$, (ii) $t = 0.5$, (iii) $t = 1$.

Fig. 7 displays the contour of H_z computed using the S-FDTDI scheme (left column) and the F-FDTDII scheme (right column) at time $t = 0.2$, 0.5 and 1 with the spatial step sizes $\Delta x = \Delta y = 10^{-2}$ and the time step size $\Delta t = 2 \times 10^{-2}$. From this figure it can be seen that the S-FDTDII scheme is more stable (and more accurate) than the S-FDTDI scheme since the perturbation error in the S-FDTDI scheme is bigger than that in the S-FDTDII scheme.

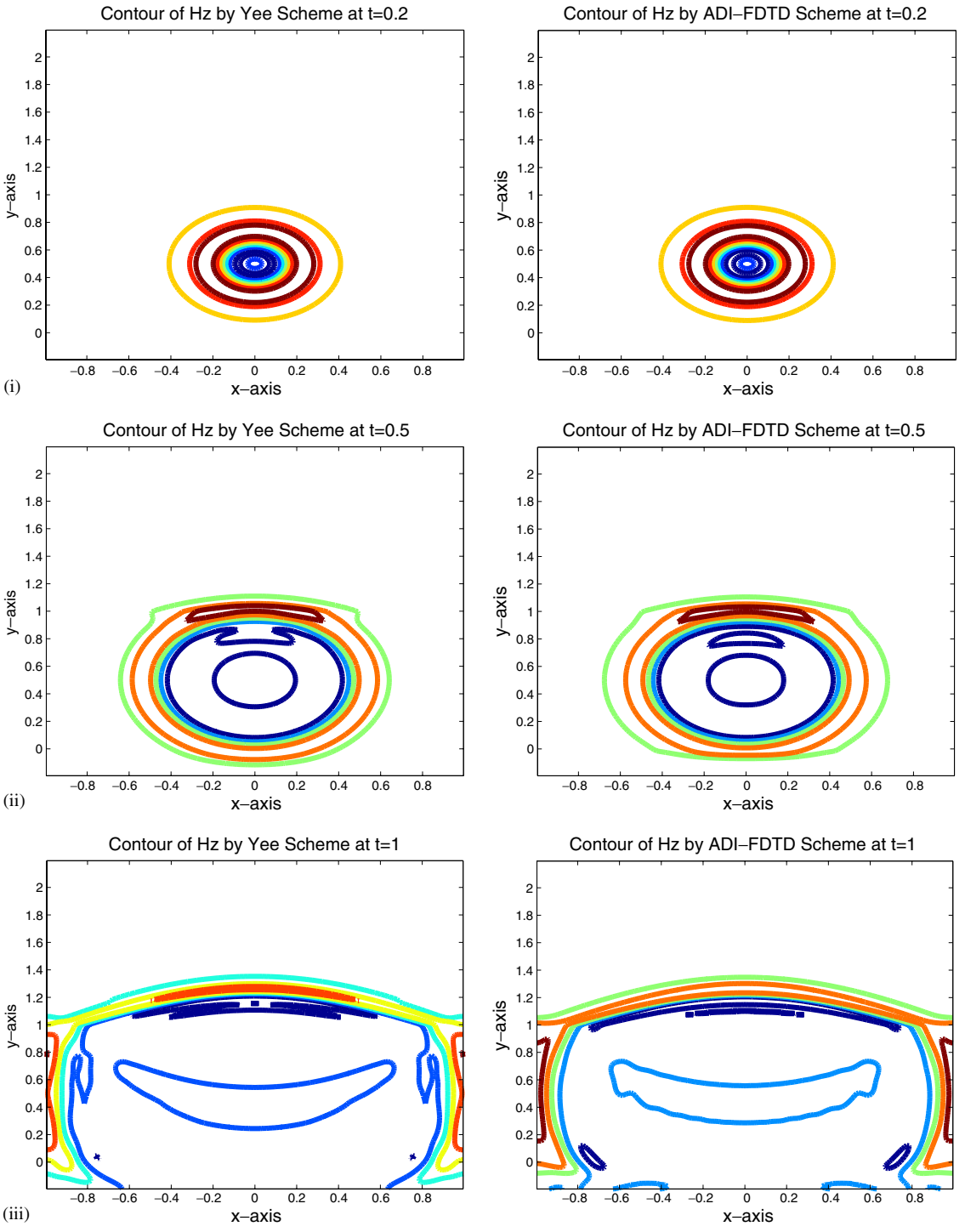

Fig. 8. Contour of H_z by Yee's scheme (left, $\Delta t = 0.2h$) and 2D-ADI-FDTD (right, $\Delta t = 2h$) with $h = 0.01$. (i) $t = 0.2$, (ii) $t = 0.5$, (iii) $t = 1$.

Fig. 8 gives the contour of H_z by Yee's scheme (left column, $\Delta t = 0.2 \times 10^{-2}$) and the 2D-ADI-FDTD scheme (right column, $\Delta t = 2 \times 10^{-2}$) with the same spatial step sizes as in Fig. 7. Comparing this figure with Fig. 7, it is found that the numerical solutions computed using the S-FDTDII scheme, Yee's scheme and the 2D-ADI-FDTD scheme are in

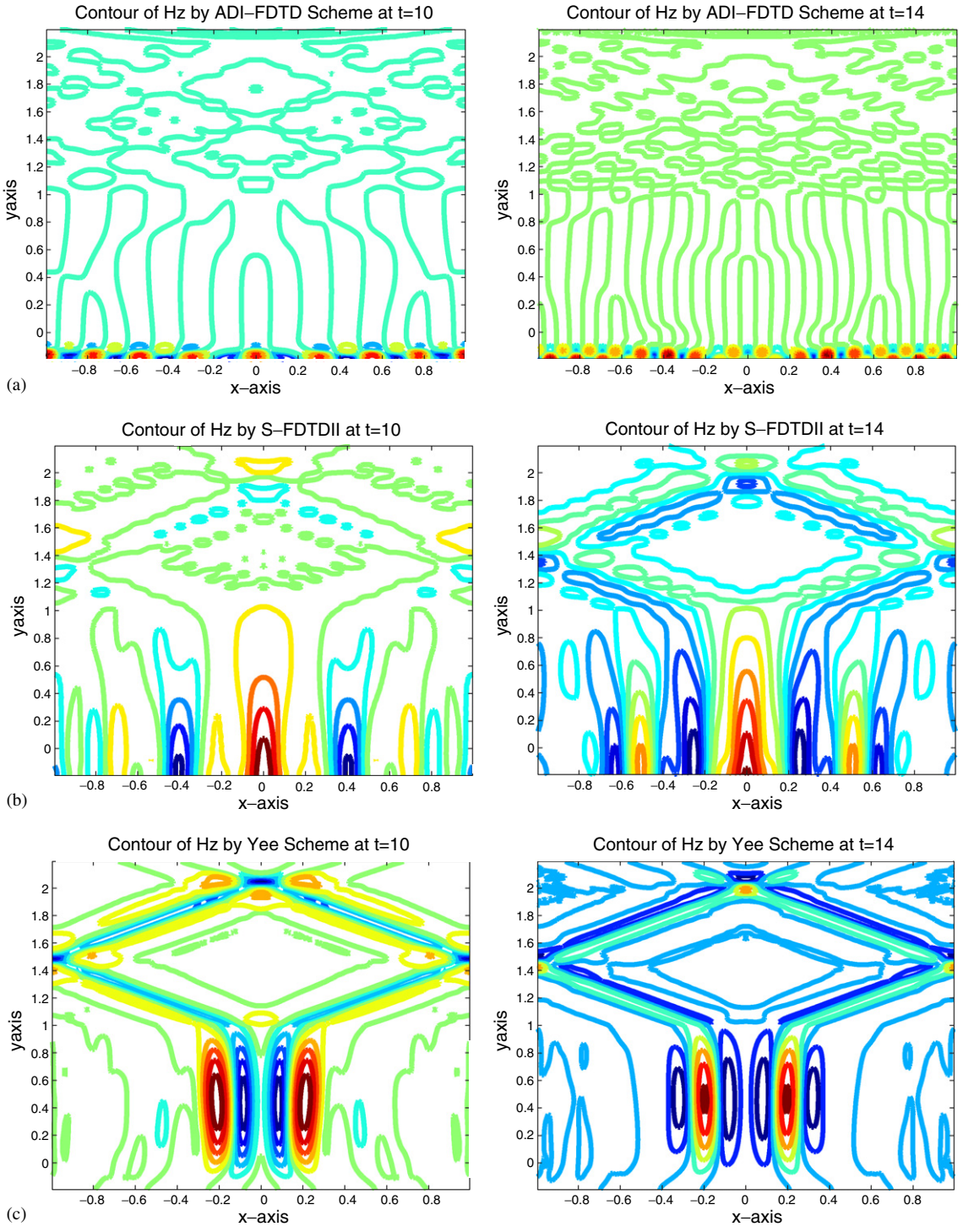

Fig. 9. Contour of H_z at $t = 10$ (left) and $t = 14$ (right) by (a) 2D-ADI-FDTD ($\Delta t = 2h$), (b) S-FDTDI ($\Delta t = 2h$) and (c) Yee's scheme ($\Delta t = 0.2h$), where $h = 0.01$. (a) By 2D-ADI-FDTD, (b) by S-FDTDII, (c) by Yee's scheme.

good agreement for small time. This confirms that the S-FDTDII scheme is efficient in solving this kind of scattering problems and that the S-FDTDII scheme has the same accuracy as the 2D-ADI-FDTD scheme. On the other hand, the S-FDTDII scheme saves much computational time than the 2D-ADI-FDTD scheme does, and the S-FDTDII scheme has better stability property than the 2D-ADI-FDTD scheme in a long time computing, as shown clearly in Fig. 9. Fig. 9 presents the contour of H_z at $t = 10$ (left) and 14 (right) computed using (a) the 2D-ADI-FDTD scheme with $\Delta t = 2 \times 10^{-2}$, (b) the S-FDTDII scheme with $\Delta t = 2 \times 10^{-2}$ and (c) Yee's scheme with $\Delta t = 0.2 \times 10^{-2}$, where the spatial step sizes are taken as $\Delta x = \Delta y = 10^{-2}$. From Fig. 9 it is clearly seen that the numerical results computed using the S-FDTDII scheme and Yee's scheme are in good agreement and are much better than those computed by the 2D-ADI-FDTD scheme at large time (e.g., $t = 14$).

As shown from Figs. 7–9, the reflected and transmitted wavefronts at the dielectric interface are clearly seen in the four methods and so is the absorption in the PML sponge layer for small time. However, for large time (e.g., $t = 14$) the wavefronts at the dielectric interface and the absorption in the PML layer are clearly seen in the S-FDTDII and Yee schemes but not in the 2D-ADI-FDTD scheme. Note that there are transmitted waves entering the region from both sides of the computational domain due to the use of periodic boundary conditions on the left and right boundaries. No instability was observed in the numerical computations.

Acknowledgments

The authors thank the referees and the editor for their invaluable comments and suggestions which helped improve the paper greatly. The work of B. Zhang was supported by the Chinese Academy of Sciences through the Hundred Talents Program. The work of D. Liang was supported by the Natural Sciences and Engineering Research Council of Canada.

References

[1] J.E. Dendy Jr., G. Fairweather, Alternating-direction Galerkin methods for parabolic and hyperbolic problems on rectangular polygons, SIAM J. Numer. Anal. 12 (1975) 144–163.
[2] J. Douglas, T. Dupont, Alternating-direction Galerkin methods on rectangles, in: B. Hubbard (Ed.), Proceedings of Symposium on Numerical Solution of Partial Differential Equations, vol. II, Academic Press, New York, 1971, pp. 133–214.
[3] J. Douglas Jr., S. Kim, Improved accuracy for locally one-dimensional methods for parabolic equations, Math. Models Methods Appl. Sci. 11 (2001) 1563–1579.
[4] J. Douglas, H.H. Rachford, On the numerical solution of heat conduction problems in two and three space variables, Trans. Amer. Math. Soc. 82 (1956) 421–439.
[5] L. Gao, B. Zhang, D. Liang, Analysis of an ADI finite difference method for the time dependent Maxwell's equations in 3-D, in: Advances in Scientific Computing and Applications, Science Press, Beijing, 2004, pp. 171–180.
[6] S.G. Garcia, T.W. Lee, S.C. Hagness, On the accuracy of the ADI-FDTD method, IEEE Antennas and Wireless Propagation Lett. 1 (2002) 31–34.
[7] S.D. Gedney, G. Liu, J.A. Roden, A. Zhu, Perfectly matched layer media with CFS for an unconditional stable ADI-FDTD method, IEEE Trans. Antennas and Propagation 49 (2001) 1554–1559.
[8] R. Holland, Implicit three-dimensional finite differencing of Maxwell's equations, IEEE Trans. Nucl. Sci. 31 (1984) 1322–1326.
[9] R. Leis, Initial Boundary Value Problems in Mathematical Physics, Wiley, New York, 1986.
[10] T. Namiki, A new FDTD algorithm based on alternating direction implicit method, IEEE Trans. Microwave Theory Tech. 47 (1999) 2003–2007.
[11] T. Namiki, K. Ito, Investigation of numerical errors of the two-dimensional ADI-FDTD method, IEEE Trans. Microwave Theory Tech. 48 (2000) 1950–1956.
[12] D.W. Peaceman, H.H. Rachford, The numerical solution of parabolic and elliptic difference equations, J. SIAM 42 (1955) 28–41.
[13] P.G. Petropoulos, L. Zhao, A.C. Cangellaris, A reflectionless sponge layer absorbing boundary condition for the solution of Maxwell' equations with high-order staggered finite difference schemes, J. Comput. Phys. 139 (1998) 184–208.
[14] A. Taflove, M.E. Brodwin, Numerical solution of steady-state electromagnetic scattering problems using the time-dependent Maxwell's equations, IEEE Trans. Microwave Theory Tech. 23 (1975) 623–630.
[15] A. Taflove, S. Hagness, Computational Electrodynamics: The Finite-Difference Time-Domain Method, second ed., Artech House, Boston, MA, 2000.
[16] Z.Q. Xie, C.H. Chan, B. Zhang, An explicit four-order staggered finite-difference time-domain method for Maxwell's equations, J. Comput. Appl. Math. 147 (2002) 75–98.
[17] K.S. Yee, Numerical solution of initial boundary value problems involving Maxwell's equations in isotropic media, IEEE Trans. Antennas and Propagation 14 (1966) 302–307.
[18] A.P. Zhao, Analysis of the numerical dispersion of the 2-D alternating-direction implicit FDTD method, IEEE Trans. Microwave Theory Tech. 50 (2002) 1156–1164.

[19] L. Zhao, A.C. Cangellaris, GT-PML: generalized theory of perfectly matched layers and its application to the reflectionless truncation of finite-difference time-domain grids, IEEE Trans. Microwave Theory Tech. 44 (1996) 2555–2563.
[20] F. Zheng, Z. Chen, Numerical dispersion analysis of the unconditionally stable 3D ADI-FDTD method, IEEE Trans. Microwave Theory Tech. 49 (2001) 1006–1009.
[21] F. Zheng, Z. Chen, J. Zhang, Toward the development of a three-dimensional unconditionally stable finite-difference time-domain method, IEEE Trans. Microwave Theory Tech. 48 (2000) 1550–1558.